Oahu Distributed PV Grid Stability Study
Part 2: System Frequency Response to Load Rejection Events

Prepared for the

U.S. Department of Energy
Office of Electricity Delivery and Energy Reliability

Under Cooperative Agreement No. DE-EE0003507
Hawai'i Energy Sustainability Program

Task 2: Energy Modeling and Scenario Analysis

Prepared by

GE Energy Consulting

Submitted by

Hawai'i Natural Energy Institute
School of Ocean and Earth Science and Technology
University of Hawai'i

May 2016

Oahu Distributed PV Grid Stability Study

Part 2: System Frequency Response to Load Rejection Events

Prepared for: Hawaii Natural Energy Institute

Prepared by: GE Energy Consulting

Date: May 31, 2016

Foreword

In the fall of 2015, GE Energy Consulting and the Hawaii Natural Energy Institute began a technical assessment of the Oahu power grid, with a goal of utilizing power system models to understand and quantify the impact of increasing variable renewable energy technologies, specifically distributed photovoltaic (DPV) energy, on system stability, reliability, and economics.

This report is the second part of a multi-faceted project that will cover several topics of renewable integration. This report outlines the methodology, analysis and key findings of the analysis related to "Part 2: System Frequency Response to Load Rejection Events." It follows the same approach as "Part 1: System Frequency Response to Generator Contingency Events." In many ways it is the inverse of the previous analysis, evaluating over-frequency events rather than under-frequency events. The underlying production cost simulations and challenging hour selection are consistent between the two study parts. The results and charts in this report are intended to complement the first part. Some material is repeated to allow the reports to be read and understood in isolation of one-another.

While this report is meant to be a stand-alone document and can be read independently of the other project parts, it should be viewed in a larger context. This report will not address all questions or topics related to grid stability and renewable integration, but will refer readers to additional scope that will be the subject of future analysis.

This report was prepared by General Electric International, Inc. ("GEII"); acting through its Energy Consulting Group ("GE Energy Consulting") based in Schenectady, NY, and submitted to the Hawaii Natural Energy Institute ("HNEI"). Questions and any correspondence concerning this document should be referred to:

Technical Contact

Derek Stenclik

Manager, Power Systems Strategy

GE Energy Consulting

General Electric International, Inc.

One River Road

Building 53

Schenectady, New York 12345

Phone: 434-978-5052

Fax: (518) 385-5703

E-Mail: derek.stenclik@ge.com

Project Team

GE Energy Consulting

Derek Stenclik

Matthew Richwine

Richard Piwko

Hawaii Natural Energy Institute

John Cole

Richard Rocheleau

Kevin Davies

Technical Review Committee

Hawaii Public Utilities Commission (HPUC)

Hawaiian Electric Company (HECO)

Department of Business, Economic Development, and Tourism (DBEDT)

Division of Consumer Advocacy

Brendan Kirby

Sebastian Nola

Note: While the Technical Review Committee was involved in regular status update meetings and reviews of the project methodology, the findings and results presented in this analysis does not constitute endorsement by the parties listed above.

TABLE OF CONTENTS

LIST OF FIGURES

LIST OF TABLES

1 INTRODUCTION

1.1 Study Overview & Objectives

The electric power industry in Hawaii is at a critical nexus; renewable technologies such as wind and solar are a rapidly growing portion of the islands' overall energy mix, the Hawaii State Legislature recently passed the country's most progressive renewable energy policy (requiring 100% of electricity to be produced by renewable technologies by 2045), and the state's primary utility, the Hawaiian Electric Company (HECO), is currently involved in a merger and acquisition. As a result, Hawaii's power grids are transforming quickly. At the end of 2015, the Oahu grid had over 343 MW of distributed solar PV (DPV) systems,[1] leading the nation in distributed solar adoption and continuing to grow. At the same time, the Hawaii Public Utilities Commission (PUC) approved approximately 140 MW of additional utility-scale solar PV projects, which may come online before the end of 2017.

With considerable changes taking place on the system, robust engineering and economic planning studies are critical. There are several ongoing analyses and modeling efforts underway or recently completed addressing renewable integration plans and challenges. Most notably, HECO is performing additional analysis required for the Power Supply Improvement Plan,[2] which outlines the utility's long-term outlook with specific attention towards renewable integration efforts. Additional production cost and long-term planning analyses, including those performed by GE Energy Consulting and the Hawaii Natural Energy Institute (HNEI), have focused on the annual and hourly impact of renewables on system operations and economics.

While production cost and capacity expansion studies are a necessary part of system planning, they do not evaluate the dynamic performance of the grid during critical operating periods and contingency events. This second type of analysis, dynamic simulation, focuses on the grid's performance over the course of seconds, or fractions of seconds, in response to randomly occurring grid disturbance events such as generator trips, loss of load, or transmission system faults. It is important to evaluate and understand the grid's dynamic performance because as wind and solar integration increases, there is a potential for the grid's dynamic performance to erode. If this occurs, the grid will be more vulnerable to critical disturbances and may increase the likelihood of an island-wide grid blackout. This is because wind and solar generators are fundamentally different from conventional thermal synchronous machines. As wind and solar begin to displace conventional thermal generators, the system may lose important ancillary services to maintain the grid's dynamic performance. While wind and solar can provide many of these critical services it will require a shift in grid operations and better understanding of their impacts on frequency response.

---

[1] Hawaiian Electric Company, "Quarterly Installed PV Data, 4th Quarter 2015," https://www.hawaiianelectric.com/clean-energy-hawaii/going-solar/more-solar-information

[2] Hawaiian Electric Company, "Power Supply Improvement Plan," HPUC Docket 2014-0183, Commission Order No. 33320, February 16, 2016.

In addition, much of the dynamics work that was done in the past focused on a select few number of operating points, often evaluating only the very extremes of system operation. While it is necessary to ensure grid stability and reliability at all times, it is important to understand the regularity and magnitude of critical operating periods. This understanding will ensure that mitigations to prevent or avoid grid stability challenges will be properly evaluated. For example, low-probability events may be best addressed using changes to operating practices or even under-frequency load shedding because the probability of occurrence is low, whereas high-probability events may be better addressed with new technologies and capital investments.

To address the need for additional analysis, this study was performed to evaluate the stability and dynamic performance of the Oahu power grid with increasing levels of renewable penetration, with a particular emphasis on the growth of distributed photovoltaic (DPV) solar resources. DPV was the primary focus of this study because it is the fastest growing renewable energy resource in Hawaii, is currently uncontrolled by the grid operator, and currently does not provide frequency response services to the grid. This part of the study focuses on the system's frequency response to a large loss of load event (load rejection contingency) only. The analysis on loss of generation contingency events was evaluated in Part 1 of this study, while other aspects of grid stability, including grid strength, will be evaluated in later stages of analysis and documented in upcoming reports.

The novel approach implemented in this study attempts to provide a better link between the dynamic grid simulations and the production cost analysis. To do this, the study created a composite frequency stability metric that can be used to quantify the level of risk to major system disturbances over _**all**_ hours of the year in contrast to traditional methods, which typically evaluate only an isolated selection of dispatch conditions or "snapshots" over the course of a year. This was achieved by a careful examination of key variables associated with grid frequency response, and a close calibration of this composite metric to the outputs of dynamic simulations. This is the same methodology as the Part 1, generator contingency analysis, but uses slightly different indicators and weighting factors.

The remainder of this report discusses the methodology of the analysis, analytical results of modeling simulations, potential mitigation strategies, and key observations for Oahu's frequency response with increasing DPV.

1.2 Overview of Frequency Response

A common characteristic of all power grids is the requirement that generation (supply) and system load must be balanced at all times. This balance is measured by system frequency. North American and Hawaiian power grids operate at a nominal frequency of 60 Hz. If generation is higher than load, frequency rises above 60 Hz; if generation is lower than load, frequency declines below 60 Hz. Given that the load on the system is constantly changing throughout the day, generation resources must constantly adjust their output to regulate grid frequency back to 60 Hz. PV generation, which changes its output as a function of irradiance from the sun, further complicates this situation because it adds more variability to the balance of generation and load, and thereby puts more duty on generators that can regulate frequency and maintain balance.

While minor fluctuations in grid frequency are normal and expected, large deviations are a risk to grid stability. Loads and/or generators may begin to trip offline and grid collapse (black-out) becomes a possibility.

It is particularly important that frequency be properly regulated in response to critical emergency events. For example, if a distribution feeder trips offline, the power system loses load immediately and system frequency increases rapidly. These changes occur within a few seconds and corrective actions must be taken within those few seconds to restore balance and avoid a grid collapse. While large load rejection events are rare and infrequent, the grid operator must manage the grid to prepare for such events. Generally speaking, when a loss of load event occurs the online generating units quickly decrease output to restore balance. This is controlled by the generator's governor, which automatically detect a grid disturbance and change output accordingly.

As generators decrease their output, the increase in frequency slows and ultimately the frequency begins decreasing back towards 60 Hz. This inflection point is referred to in this report as the frequency zenith and is the highest point in system frequency following a load contingency event. Over the course of about 30 seconds, the system will stabilize at a new quasi-equilibrium settling point. The change in power output from controlled resources (mostly generators) is called frequency response. Figure 1 provides an illustrative example of system frequency during a large load rejection event with the following points demarcated:

- **A:** Initial condition, system is stable at nominal frequency of 60 Hz, load rejection event occurs at time = 10 seconds.
- **A→C:** Frequency increases rapidly because system generation exceeds load.
- **C:** System frequency eventually stops increasing at the zenith (C) when generation resources decrease their output to restore balance between load and generation.
- **C→B:** System frequency "backswings" as generators with governors continue to respond to the event and regulate the system frequency back towards 60 Hz.
- **B:** System recovers to a new stable equilibrium. The new equilibrium at 30 seconds may not be equal to the initial condition (60Hz). The final restoration to 60 Hz normally takes a little longer, through the operation of automatic generation control (AGC) or by re-dispatch of thermal units.
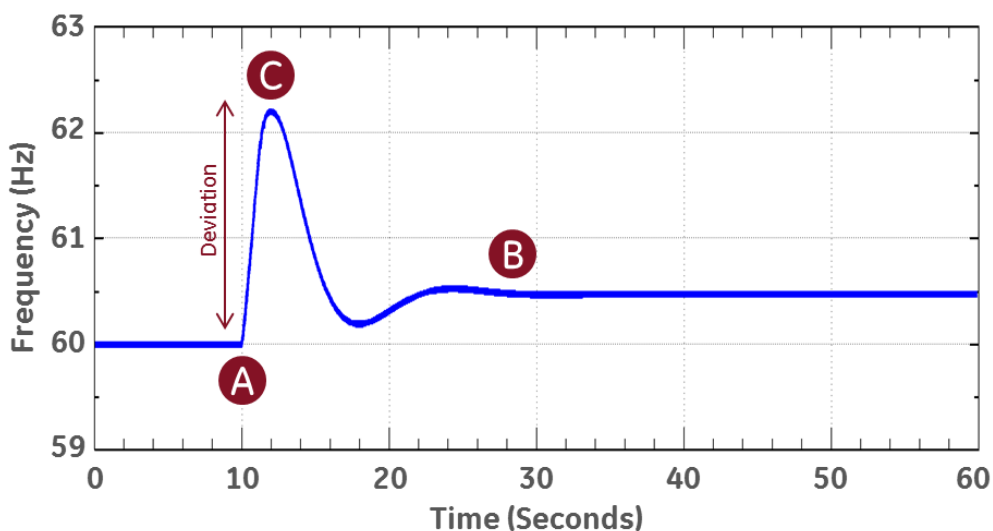
Figure 1: Illustrative Example of System Frequency Response to a Load Rejection Event

As is the case with many island power grids, the Oahu grid is unique relative to large interconnected power systems. A relatively small fluctuation in either generation or load can lead to large, and potentially unstable, deviations in system frequency for several reasons;

1. **Large Single Contingency:** Oahu's largest anticipated load rejection event is about 10% of total system load. It is based on the unlikely, but possible, tripping of several load feeders in close proximity to each other by a common initiating event. The magnitude (MW) of this event varies from hour to hour since system load is higher during daytime hours and lower during nighttime hours. The magnitude of the loss of load event defines the hourly down-reserve requirement maintained by the system operator.

2. **Low number of synchronous generators**: Relative to large interconnected grids, Oahu has a low number of synchronous generators online and available to provide primary frequency response. In addition, some generators like H-Power do not have governors enabled and therefore do not provide primary frequency response.

3. **No interconnections to neighboring systems:** The Oahu power grid is an isolated system. Large interconnected grids in North America can lean on neighbors during contingency events for support. Hawaii does not have this luxury and must provide all frequency response locally from on-island resources.

4. **High Level of Distributed PV Penetration:** The Oahu grid has very high penetration of DPV. While many of the DPV inverters have been upgraded to include frequency ride-through capability, there is currently no mechanism or control system to provide over-frequency droop response (also referred to as frequency-watt autonomous control). Therefore, as solar penetration increases, thermal units will be backed down to lower loading levels, reducing down-reserves available to respond to a load rejection event.

As a result, the Oahu grid operators rely exclusively on governor response from online thermal generating units during contingency events. As the amount of wind and solar

capacity on the system increases, thermal units online will be cycled off or reduced to lower loading levels. This will erode the system's capability to respond to over-frequency events. If the magnitude of the frequency deviations increases too much, generator protections will engage and potentially trip units off-line. If this occurs, an over-frequency event caused by a load rejection can quickly cause a loss-of-generation contingency and cascade into an under-frequency event. As a result, the load rejection event has the possibility to cause under-frequency load shedding (UFLS) and eventually a grid collapse or blackout event, if the system's governor response not able to quickly compensate for the reduction in system load.

Thus, it is critical to understand the impact of increasing DPV on Oahu's system frequency response and to better understand alternative tools and mitigations available to the utility to enhance grid stability. These may include frequency response provision from variable renewable energy sources (both utility-scale and distributed), energy storage, electric vehicles, and demand response.

1.3 Scope & Limitations

While this study significantly expands the technical analysis into areas not examined in previous studies, it is not exhaustive in covering all possible risks and mitigations for grid frequency stability. In particular the following points highlight the scope and potential limitations of the study:

- This study does not replace existing analysis conducted by the utility, state regulators or other stakeholders in Hawaii. Instead, it is intended to supplement those studies with additional technical analysis and findings.

- This study evaluated load rejection contingencies only. It did not evaluate other important aspects of grid stability such as generator contingency events, transmission faults, or short-circuit strength. This report represents Part 2 of a broader ongoing project that evaluates additional aspects of grid stability and renewable integration. Part 1 addresses generator tripping contingencies in more detail.

- This study evaluated grid operations on Oahu only and did not perform simulations on other islands. Oahu was the focus of this study because it is the primary load center of Hawaii (over 70% of the state's electricity demand) and thus will require substantial renewable capacity additions in order to comply with the state's RPS targets.

- This study evaluated variable renewable capacity up to 974 MW (124 MW of wind, 150 MW of utility-scale solar and 700 MW of DPV). While this represents a substantial increase over today's installed renewables, findings should not be extrapolated beyond this level of renewable integration. Grid stability and operational challenges are non-linear and will require additional analyses to better understand higher penetration levels.

- This study analyzed system operation at the bulk-transmission grid level. It did not analyze individual distribution feeders or the circuit loading issues that may result from high levels of distribution-connected rooftop PV systems.

- The study is based on fundamental frequency, positive sequence analytical tools and models. While these are the basic and appropriate tools for analysis of frequency response, not all aspects of the dynamic performance and stability of inverter-based resources, including PV generation, are captured by them. Other types of high frequency and high bandwidth instabilities could conceivably present risks.

2 METHODOLOGY

2.1 Analytical Process & Modeling Tools

To analyze the impact of increasing DPV penetration on system frequency response, a variety of models and statistical techniques were employed in this analysis to simulate both system operations and dynamic grid stability. While these models are not measuring real system conditions, they have been routinely benchmarked and validated against historical operations and are consistent with engineering and operating practices utilized by HECO and other industry stakeholders. The methodology employed in this analysis included five steps, as illustrated in Figure 2. Please note that the production cost simulations and the selected dispatch conditions passed to the dynamic stability simulations are identical to those in the Part 1 System Frequency Response to Generator Contingency Events. This allows for a direct comparison of dispatch and system conditions between these two parts of the study.

Figure 2: Analytical Process

Step 1 - Production Cost Simulations (GE MAPS): The first step in the analysis was to conduct detailed hourly production cost simulations. The GE-MAPS production cost model simulates the power system operation on an hourly, chronological basis over the course of the year. The model simulates the system operator's unit commitment (on or offline) and dispatch (MW output) decisions necessary to supply the electricity load in a least cost manner, while appropriately reflecting transmission flows across the grid and simultaneously preparing the system for unexpected contingency events and variability. The chronological modeling is crucial to understanding renewable integration because it simulates chronological changes to electrical load and the underlying variability and forecast uncertainty associated with wind and solar resources.

This modeling was performed for two scenarios, along with intermediate steps (described in Section 2.2), with increasing levels of DPV penetration. This step is an essential part of the analysis because as solar penetration increases, the model provides accurate changes in hourly unit commitment, dispatch, spinning reserves and potential curtailment. The 8,760 hourly results from the production cost modeling are provided in Section 3.1 and the outputs were passed to Step 2 for further analysis.

Step 2 – Selecting System Dispatch Conditions for Dynamic Simulations: The second step in the analysis included a detailed review of the production cost simulations. This process selected specific system dispatch conditions that were passed from the production cost results to the dynamic frequency response simulations. To do this, three key variables were

analyzed for each hour of simulation: size of the largest load contingency (assumed to be 10% of load), the amount of committed capacity with governor response enabled, and the amount of spinning down-reserve provided by conventional thermal generators. These three variables were then translated to a single numerical metric quantified for each hour and dispatch condition. The metric quantifies the expected magnitude of over-frequency response for a load rejection in each hour of the year. This analysis was performed for all study scenarios, with increasing DPV penetration. Several representative hours and dispatch conditions (including load and unit dispatch) were then selected to be analyzed in greater detail in Step 3.

Step 3 – Dynamic Frequency Response Simulations (GE PSLF): Each of the hours selected in Step 2 were evaluated in greater detail through dynamic frequency response simulations using the GE PSLF model. Using the dispatch conditions provided by Step 2, including system load and unit generation, a loss of load contingency event was simulated. To do this, the GE PSLF model simulated a trip of the largest load contingency in each hour selected (assumed to be 10% of system load) and measured the system response over the course of 60 seconds. Key parameters evaluated in this part of the analysis included frequency zenith (Hz), frequency deviation (difference between the steady state frequency and the zenith, Hz), and the change in power output from online generators (MW).

Step 4 – Estimating Frequency Response for all Dispatch Conditions: In the fourth step of the analysis, the results calculated in Step 3 were statistically evaluated to examine the relationship between the calculated metric (from Step 2) and the system's frequency zenith. A polynomial regression was then estimated using the frequency zenith as the dependent variable and the metric as the independent variable. The resulting equation was then used to estimate the frequency deviation for each hour and dispatch condition of the year, across both Scenarios. This allows for a more complete picture of system risk, including the distribution of different risk levels over the course of the year and a comparison with increasing DPV scenarios.

Step 5 – Analyze Potential Mitigations to System Frequency Response: The fifth and final step of the analysis included the evaluation of potential mitigations to improve system frequency response. While there are many options available to the system operator, this study evaluated two sensitivities that included frequency response (governor droop) from additional assets;

- Existing thermal generators and utility scale wind and solar plants,
- Existing thermal generators, utility-scale wind and solar plants, and DPV.

Using the same selection of hours and dynamic simulations used in Step 4, this section allows for a direct comparison of system frequency response using a larger pool of assets providing governor response.

2.2   Scenario Overview

To evaluate the impact of DPV on grid stability, two scenarios were evaluated. Scenario 1 included 400 MW of installed DPV capacity and Scenario 2 had 700 MW of DPV installed. Note that intermediate scenarios were evaluated with incremental 100 MW DPV capacity additions, but only the scenarios with the lowest and highest installed DPV are discussed in this report. Scenario 1 represents the likely installed DPV capacity online by 2017, assuming a continuation of recent trends. Scenario 2 was analyzed to show the impact of increased DPV penetration and was identified as a system hosting capacity limit in a recent PUC docket filing.[3] The hourly chronological solar output profiles were scaled linearly between the two scenarios, and the spinning reserve requirements were adjusted accordingly (see section 2.3 for more information). All other inputs and assumptions were held constant across the scenarios, isolating any changes due to increased DPV penetration.

Figure 3 provides an overview of the installed renewable capacity and available energy (prior to potential curtailment) for each of the scenarios evaluated. In the absence of curtailment, annual wind and solar energy penetration would be between 16% in Scenario 1 to 22% in Scenario 2. It is important to note that while production cost simulations and hourly screening were performed on all four scenarios, only Scenario 1 and Scenario 2 were evaluated in the dynamic simulations to provide a bookend analysis and to limit the number of dynamic simulations required. In addition, the 700 MW of DPV selected in Scenario 2 is not intended to show a maximum amount of DPV on the Oahu grid, but rather to reflect potential near-term growth.

Capacity (MW)

	SCEN1	INTERMEDIATE		SCEN2
DPV	400	500	600	700
CPV	149	149	149	149
WIND	123	123	123	123

Available Energy (GWh)

	SCEN1	INTERMEDIATE		SCEN2
DPV	635	794	953	1111
CPV	282	282	282	282
WIND	356	356	356	356
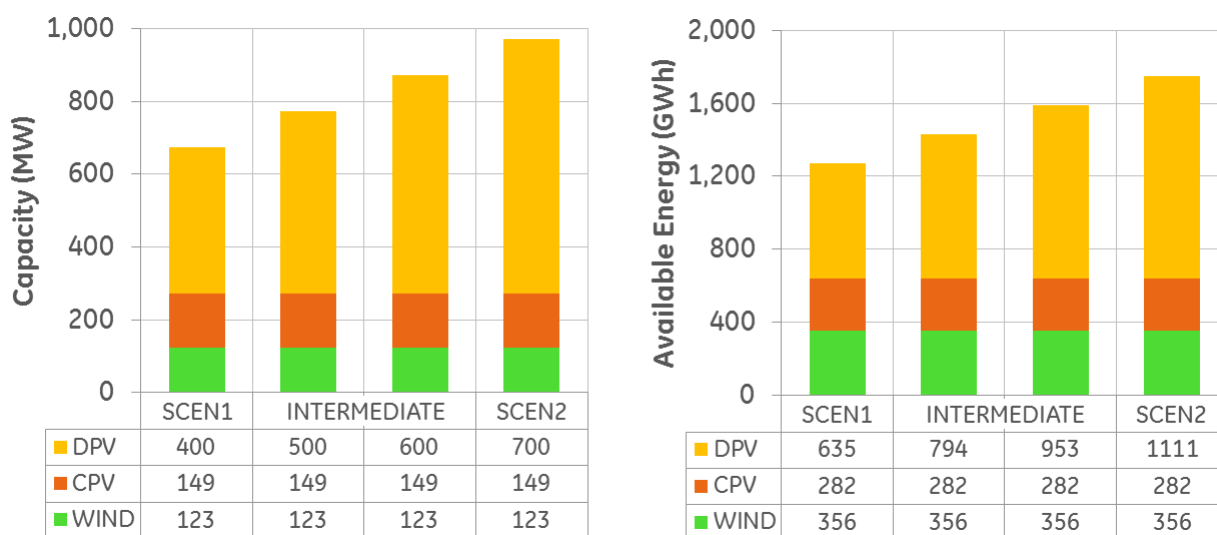
Figure 3: Installed Wind & Solar Capacity & Available Energy by Scenario

---

[3] Hawaiian Electric Company, "System Level Hosting Capacity," HPUC Docket 2014-0192, Commission Order No. 33258, December 11, 2015.

2.3 Inputs & Assumptions

The inputs and assumptions used throughout the modeling efforts were developed in close collaboration with other modeling efforts in Hawaii, including previous studies conducted by GE Energy Consulting and the HECO Power Supply Improvement Plans. GE Energy Consulting coordinated with HECO to ensure that all inputs and assumptions were current and utilizing the best available data. The following section provides an overview of high-level assumptions.

The GE MAPS production cost simulations included a detailed, nodal representation of the Oahu system, including:

- Distributed PV: 400 MW in Scenario 1, increasing to 700 MW in Scenario 2.
- Utility-scale PV: 11 MW of existing solar plus approximately 140 MW of Waiver PV projects with PUC approval.
- Utility-scale Wind: Existing 99 MW of wind (Kahuku (30) and Kawailoa (69) wind plants), plus the proposed 24 MW Na Pua Makina wind plant.
- Wind and Solar Profiles: Hourly simulated production profiles for the year 2008, created for the Hawaii Solar Integration Study.
- Thermal generators: Current operating plants as of January 1, 2016 without any new installations or retirements (AES, Kahe 1-6, Kalaeloa CC, Waiau 2-10, CIP CT, Airport Biodiesel, and H-Power). Each generator was modeled with a high degree of fidelity, including maximum and minimum stable operating capacities (MW), incremental heat rate curves (btu/KWh), variable operations & maintenance costs ($/MWh), and cycling constraints.
- Spinning Reserves: 180 MW of contingency reserves plus regulation reserves required for wind and solar variability.
- Thermal Unit Flexibility: Lower minimum stable operating levels (P-Min) on Kahe 1-4, and Waiau 7-8 consistent with the PSIP. Unit cycling (removed must-run constraints) allowed on Kahe 1-4.
- Load: Annual energy of 7,959 GWh and a peak demand of 1,223 MW.
- Fuel Price: $60/bbl of oil, adjusted to include refining delivery charges for a 70/30 LSFO-Diesel fuel blend for each unit.

One of the most important inputs and assumptions in the analysis is the minimum loading level for the existing thermal units (operational P-Min). This represents the lowest MW dispatch point at which the units are allowed to operate during normal operations (production cost simulations), and thus dictates how much down-reserves are available during load rejection events (dynamic stability simulations). In practice, units are often operated at a power output that is higher than the technical P-min of the machine. This allows greater governor response during a contingency event and avoids operating at very low loads where it is more challenging to control steam turbine boilers and gas turbine combustion. While this study assumed reduced operational P-Mins on thermal units (relative to historical operations), it still included a buffer between the operational P-Min and the technical P-Min. The technical P-min is the lowest possible stable operating point for a

generator. The range between the operational P-min and the technical P-min is normally reserved for downward governor action in response to over-frequency events.

The operational and technical P-Mins are provided for each baseload thermal unit in Table 1. The operational P-Min values are used in the production cost simulation (GE MAPS model) and determine the dispatch conditions used in the dynamic simulations (GE PSLF model) where the output is permitted to decrease further during a contingency event. Note that the difference in the technical and operational P-Min on the Kalaeloa units is due to the current PPA structure and cogen requirements of the plant.

Table 1: Operational and Technical Thermal Unit P-Min

	TECHNICAL P-MIN (PLSF)	HOUSE LOADS	TECHNICAL P-MIN (PLSF)	OPERATIONAL P-MIN (MAPS)	DOWNRANGE @ P-MIN
	MWgross	MWgross	MWnet	MWnet	MWnet
AES	76.0	20.0	56.0	63.0	7.0
Kahe 1	26.0	2.2	23.8	25.0	1.2
Kahe 2	26.2	2.2	24.0	25.0	1.0
Kahe 3	26.3	2.2	24.1	25.0	0.9
Kahe 4	25.8	3.4	22.4	25.0	2.6
Kahe 5	45.0	6.2	38.8	45.0	6.2
Kahe 6	45.0	6.2	38.8	40.0	1.2
Waiau 7	26.6	3.6	23.0	25.0	2.0
Waiau 8	26.2	3.6	22.6	25.0	2.4
Kalaeloa CC1	31.0	2.0	29.0	65.0	36.0
Kalaeloa CC2	31.0	2.0	29.0	65.0	36.0

Transmission System

The underlying powerflow model utilized during the production cost and dynamics simulations was provided by HECO in PSS/E format as their 2015 load flow case. The model included the Oahu network topology and major equipment ratings like transformer ratings. The network captures the lines and buses at the 46kV level and above, with lines and buses at lower voltages included for generation plants. A simplified, high-level representation of the overall model is shown in Figure 4.
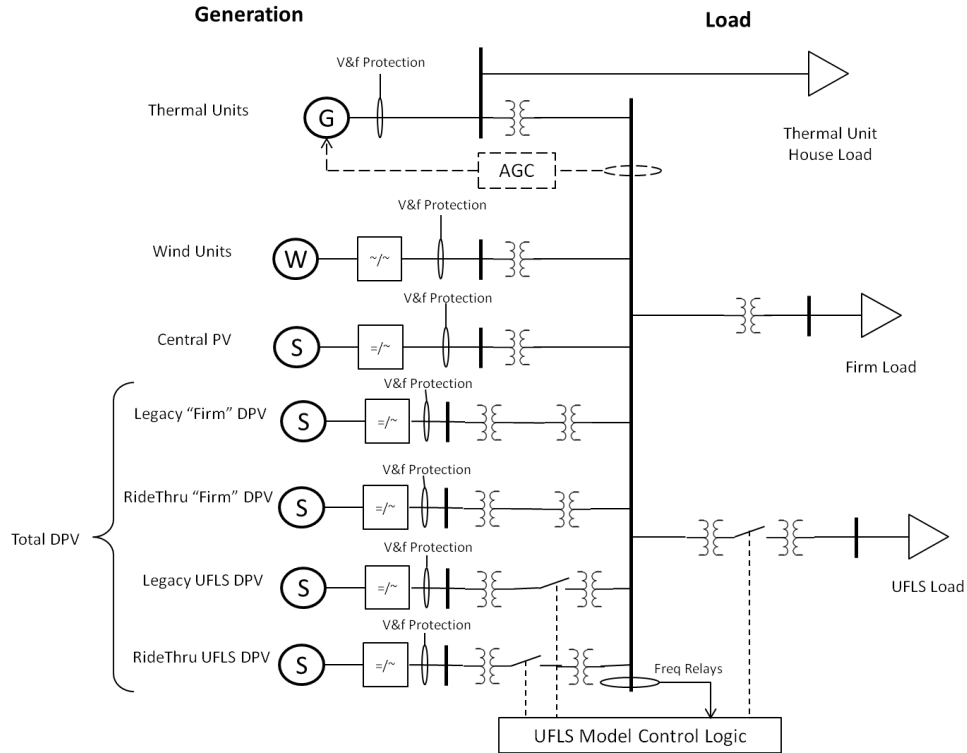
Figure 4: Overview of the Oahu Dynamic Simulation Model

Thermal Generation

For each thermal generation unit, a dynamic model that included the generator, exciter, and governor was used, based on inputs from HECO in their 2015 PSS/E Dynamics Record File (DYR). Frequency protection was modeled for the following thermal generators: Kalaeloa CC, Kahe 5-6, Waiau 7-8 with the assumed trip settings of +/-3Hz @ 2.0 seconds.

Wind Generation

Each wind plant was modeled as an aggregate plant model, with the exception of the Na Pua Makina wind farm in which each turbine was modeled individually in the original load flow received. The dynamic models included the generator, converter, and turbine where the models and parameters are assumed to be values typical of utility-scale wind turbines with low-voltage ride-through features enabled and frequency ride-through capability of +1.5Hz / -3Hz @ 6.1 seconds; +3Hz/-3.5Hz @ 0.1 seconds.

Central PV Generation

Each central PV plant was modeled as an aggregate plant model with dynamic models that are assumed to be typical of utility-scale PV plants with low-voltage ride-through features enabled and frequency ride-through capability of +1.5Hz / -3Hz @ 6.1 seconds; +3Hz/-3.5Hz @ 0.1 seconds.

Distributed PV Generation

The distributed PV generation was modeled as 31 aggregate PV plants interspersed throughout the Oahu power grid. Each of the DPV models connects to a 480V bus, where an aggregate transformer with an impedance assumed to be typical of two transformers in series connecting the 480V PV bus to the 46kV transmission system bus. A dynamic model of each DPV generator was used with settings typical of distributed PV systems.

The frequency ride-through settings were provided in the HECO model, and vary based on the classification of the DPV.

- "Legacy" DPV frequency trip settings: 59.3Hz @ 0.157 seconds; 60.5Hz @ 0.157 seconds
- "Ride-through" DPV frequency trip settings: 57.0Hz @ 0.157 seconds; 63.0Hz @ 0.157 seconds

While it is estimated by HECO that there remains 106MW installed DPV capacity with the over-frequency trip settings set to 60.5Hz and 0.157 seconds (over-frequency legacy DPV), this analysis assumes that all of the DPV will ride through an over-frequency event (up to 63 Hz).[4] The reason for neglecting the over-frequency legacy DPV is that a small loss of generation quickly following a loss of load event actually helps the grid recover from the initiating event by moving the grid closer to its new equilibrium. However, when the loss of generation approaches or exceeds the initial loss of load in magnitude, then the loss of generation is detrimental to system stability and can transform an over-frequency event into an under-frequency event that triggers under-frequency load shedding (UFLS) and can lead to system collapse. As explained in detail in Section 3.5, the 106 MW of over-frequency legacy DPV on Oahu is not enough to trigger UFLS or risk grid collapse under expected operating conditions. Therefore, it is conservative to neglect the 106 MW of DPV that does not have over-frequency ride-through settings applied.

The total DPV generation from MAPS was proportionally allocated among the 31 aggregate DPV models based on their original rating in the load flow, where the DPV was represented as a negative load. A "DPV fraction" was calculated by dividing the total DPV dispatched in the hour by the total DPV installed in the scenario.

Voltage relay settings were not implemented in the model because the events being analyzed did not involve system faults or significant voltage excursions.

Load

Static loads, with constant impedance, current, and power (commonly known as ZIP load models), were used for all system loads, which are aggregated and connect at the 46kV level. The modeled loads are frequency-dependent and the total system load was split proportionally among 38 load buses according to their dispatch in the original load flow provided by HECO.

---

[4] The estimated 106 MW of over-frequency legacy DPV is 36 MW higher than the estimated under-frequency legacy DPV because of DPV inverter upgrades took place at a later time and updated the under-frequency settings.

Generator plant auxiliary loads (house loads), provided in Table 2, at several of the generation plants were modeled explicitly. During a generator trip event, it is assumed the house loads at the plant remain on at their pre-trip power level, which is a conservative assumption.

Table 2: Summary of Generator Plant Auxiliary Loads

Generator	House Load (MW)
Kahe 1,2,3	2.2
Kahe 4	3.4
Kahe 5,6	6.2
Waiau 7,8	3.6
Kalaeloa 1,2	2.0
AES	20.0

Over-Frequency Droop

Over-frequency droop is a one-sided frequency response in which a generating unit reduces power output proportionally with the deviation of frequency from its nominal value when the frequency exceeds a defined threshold, or deadband. Below this threshold, the unit does not respond to frequency, but follows its set point as if it were in constant-power control mode. This allows generators to respond to over-frequency events like load-rejections even if they are otherwise operated in constant-power control mode.

The load rejection events under Scenario 2 were repeated with over-frequency droop added to the renewable generation plants in stages to show the effect of including over-frequency governor response on more generation sources, the results of which are presented in Section 4.

The over-frequency droop settings used in simulations of the sensitivities are outlined below:

A. No droop on the renewables
B. 2.5% droop with 36mHz deadband and a 2-second time constant on the utility-scale renewables
C. 2.5% droop with 36mHz deadband and a 2-second time constant on the utility-scale renewables and 5% droop with 36mHz deadband on the distributed PV

3 ANALYTICAL RESULTS

3.1 Production Cost Simulations

The hourly production cost simulations were performed for a chronological, 8,670 hour dispatch of the Oahu power system. This analysis takes into account the commitment and dispatch of both conventional thermal generators and wind and solar generators to serve the system load in a least cost manner. Included in the optimization are constraints on system operations including transmission constraints, fixed operating schedules of some baseload units (must-run status), spinning reserve provision for contingency events and wind and solar variability, minimum run times and down times, and generator outages.

The result of this analysis provides a chronological commitment and dispatch profile for the thermal units, delivered and curtailed wind and solar generation, total fuel consumption and production cost (fuel costs, variable operations and maintenance costs, and startup costs). The hourly simulation results were then screened for challenging hours of operation, and investigated in further detail for grid stability.

Figure 5 provides a visualization of a week of chronological system dispatch (Monday – Sunday) from the GE MAPS model output. The figure provides and illustrative example of how unit commitment and dispatch takes place over the course of a week. The upper envelope of the curve represents the total system load, while each colored band represents the output of a unit (or group of units). Thermal generating units are ranked, from the bottom up, based on their variable costs of generation and/or fixed operating schedules and must-run rules. Wind and solar generating units are shown on top. With the increased solar PV on the system, the overall change to the net load (total system load minus wind and solar power) is pronounced. During mid-day hours the baseload thermal generating units are backed down to near minimum loading levels. In addition, it can be observed that peaking units and some cycling units (Waiau 3-6) are utilized exclusively during the morning or evening hours during load ramps, or when the solar availability is lower (cloudy day). AES and H-Power, the most economic units on the system adjust output rarely.
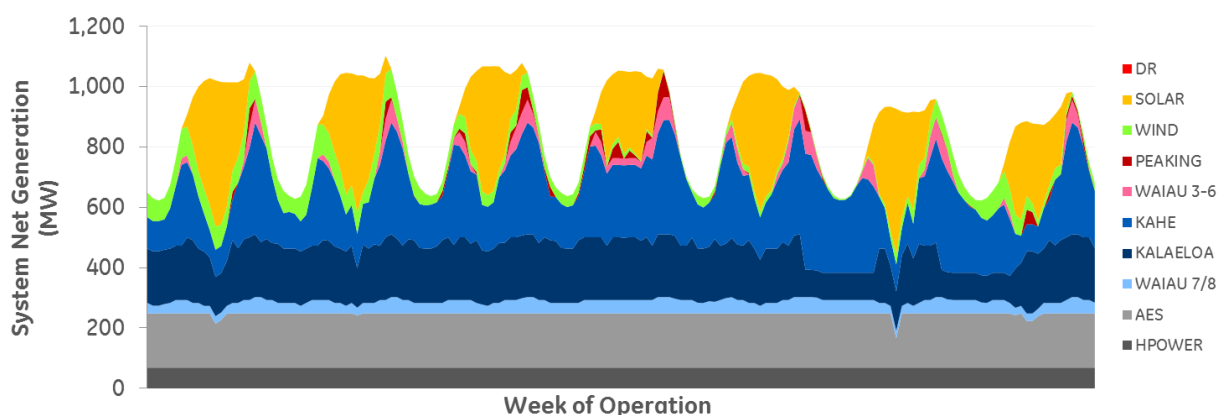
Figure 5: Weekly Chronological System Dispatch: Week 15, Scenario 1
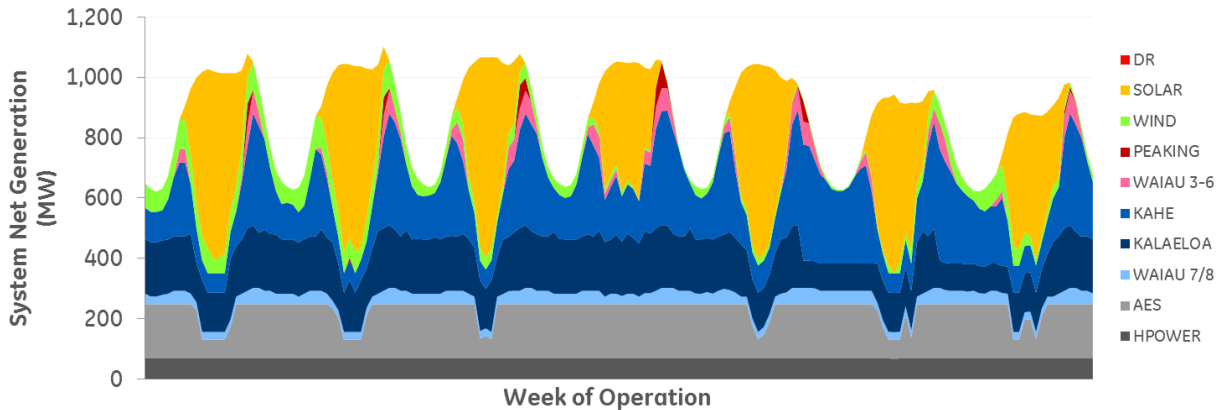
Figure 6: Weekly Chronological System Dispatch: Week 15, Scenario 2

The same week of operation is also shown in Figure 6, this time for Scenario 2, including an additional 300 MW of DPV capacity on the system. This allows for a direct comparison of the commitment and dispatch profiles across the two scenarios, isolating the impact of increased solar generation. Relative to Scenario 1, shown in Figure 5, the daily solar profiles are more pronounced, and the thermal unit cycling is increased. The thermal baseload units, shown in blue, decrease output substantially during the day-time hours, and often exhibit a flat "plateaued" operating profile. This represents times when the units are dispatched at minimum loading levels and cannot be turned down lower. If and when all units are dispatched at minimum load, the only remaining operating decision is to curtail wind or solar. In Scenario 2, even turn-down of the AES coal plant becomes a regular operating procedure.

The reduction in thermal unit output leads to significant production costs savings when replaced by wind and solar generation, but it also significantly erodes the amount of down-reserve being carried by the system if this ancillary service is only provided by the thermal units. Figure 7 compares a chronological week (same as the illustrations above) of down-reserves available from thermal units between Scenario 1 and Scenario 2. It illustrates how the reserve provision erodes during mid-day hours as more solar comes online and backs down conventional thermal units to lower loading levels.
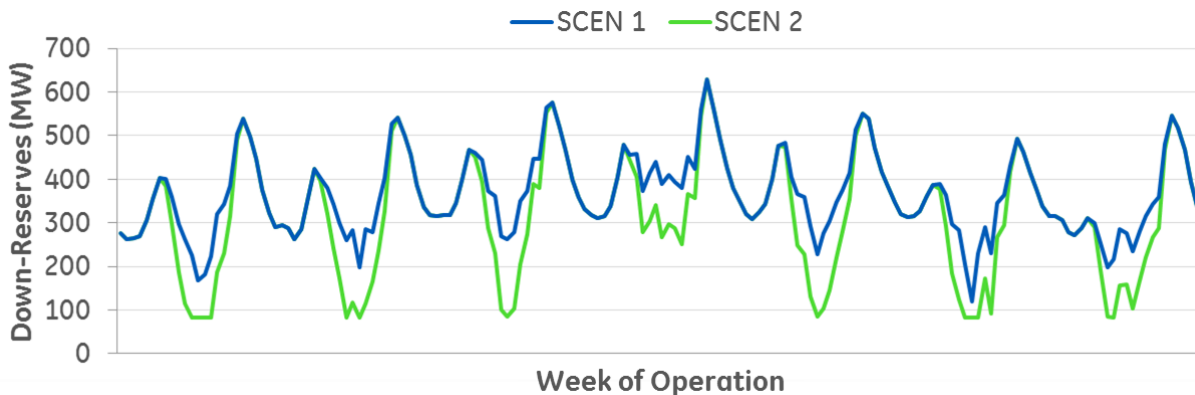
Figure 7: Weekly Chronological Down-Reserves Available: Week 15

The production cost simulation, illustrated for one week in Figure 5 and Figure 6, is continued for the full duration of the year (8760 hours). This allows for a complete screening of unit level commitment and dispatch for each hour of the year. The annual, aggregated results of this exercise are provided in Table 3 for both scenarios. From this table, several observations can be made, highlighting the changes between the two scenarios as more distributed solar is brought online.

- H-Power, AES, Kahe 5&6, Waiau 7&8, and Kalaeloa CC-1 remain in fixed operating schedules. The annual hours online and annual starts do not change between the two scenarios. However, the units are turned down more often and have a lower annual generation and capacity factor with increased DPV generation.
- Kahe 1-4, Kalaeloa CC-2 and CC-3, and Waiau 3-6 have a lower annual generation and capacity factor with increased DPV, and the number of cycles (on/off) increase. This indicates more hours of the year with decreased thermal unit commitment.
- Peaking utilization (Waiau 9-10, CIP-CT, and Airport diesel) experience a decrease in annual generation, but are required to cycle more.
- Wind and CPV plants exhibit slightly decreased generation due to increased curtailment as additional DPV is brought online.

Table 3: Annual Unit Utilization, Scenarios 1 and 2

Unit Name	Unit Type	Capacity (MW)	Scenario 1				Scenario 2			
			Generation (GWh)	Capacity Factor	Hours Online	Annual Starts	Generation (GWh)	Capacity Factor	Hours Online	Annual Starts
H-Power	ST-Waste	68.5	539.6	90%	8592	1	539.5	90%	8592	1
AES	ST-Coal	180.0	1422.4	90%	8064	1	1358.4	86%	8064	1
Kahe 1	ST-Oil	82.2	201.7	28%	4779	198	173.1	24%	4294	287
Kahe 2	ST-Oil	82.2	297.9	41%	6137	195	259.9	36%	5681	284
Kahe 3	ST-Oil	86.2	389.7	52%	7273	38	350.2	46%	7123	73
Kahe 4	ST-Oil	85.3	374.9	50%	6670	107	329.6	44%	6420	161
Kahe 5	ST-Oil	134.6	606.5	51%	5736	2	536.0	45%	5736	2
Kahe 6	ST-Oil	133.8	453.3	39%	6408	2	418.0	36%	6408	2
Waiau 7	ST-Oil	83.3	311.4	43%	7248	2	287.9	39%	7248	2
Waiau 8	ST-Oil	86.2	225.0	30%	6744	2	213.5	28%	6744	2
Kal-CC 1	CC-Oil	90.0	698.7	89%	7929	52	677.2	86%	7929	52
Kal-CC 2	CC-Oil	90.0	656.3	83%	7455	49	633.4	80%	7424	62
Kal-CC 3	CC-Oil	28.0	74.6	30%	3468	940	70.3	29%	3254	981
Waiau 3	ST-Oil	47.0	53.6	13%	1987	424	44.2	11%	1640	436
Waiau 4	ST-Oil	46.5	60.1	15%	2726	441	48.9	12%	2222	492
Waiau 5	ST-Oil	54.5	90.5	19%	4035	352	75.6	16%	3372	445
Waiau 6	ST-Oil	53.7	74.5	16%	3383	357	60.9	13%	2754	447
Waiau 9	CT-Oil	52.9	41.6	9%	1141	422	39.2	8%	1085	459
Waiau 10	CT-Oil	54.9	83.1	17%	2439	844	79.4	17%	2335	875
CIP-CT	CT-Biodsl	112.2	25.2	3%	519	225	23.8	2%	480	224
AIR-DSG	IC-Biodsl	8.0	3.7	5%	487	197	3.4	5%	454	200
Wind	Wind	123.0	355.6	33%			354.3	33%		
CPV	Solar	149.3	281.9	22%			268.8	21%		
DPV	Solar	400-700	635.1	18%			1111.5	18%		

The production cost simulation results were also analyzed on an hourly basis across the year, an important step when screening for challenging dispatch conditions. This is especially true in scenarios with increasing wind and solar penetration, due to the variable nature of the resources. Some hours of the year will exhibit high wind and solar generation on the grid while others have low or no wind and solar generation.

The range of wind and solar power output across all hours of the year is illustrated in Figure 8. These duration curves sort the hourly wind and solar output in total MW delivered and as a percent of system load from highest to lowest throughout the year. From the chart on the right it can be observed that in Scenario 1, some hours of the year approach 50% instantaneous penetration. In Scenario 2, with 300 MW additional DPV, maximum instantaneous penetration approaches 70% of system load, with approximately 1,000 hours at or above 50% instantaneous penetration. As a point of reference, EirGrid, the system operator in Ireland, has instituted limits on "simultaneous non-synchronous penetration,"[5] including HVDC imports, to 50% due to stability concerns, with curtailment required afterwards.
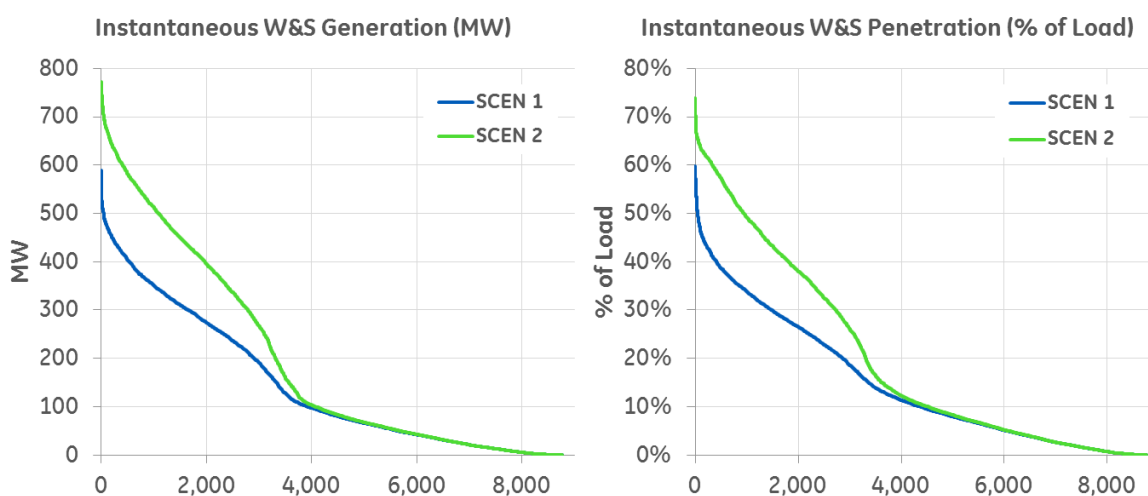
Figure 8: Hourly Duration Curves of Wind and Solar Penetration by Scenario

As discussed previously, increasing levels of DPV on the system affect several factors of system operation that are related to grid frequency performance. Figure 9 shows three of those factors; largest load contingency, the total thermal commitment (based on MW rating of online generators, not the dispatched output), and the down-reserve provision. The plots show:

- The largest load rejection contingency (assumed to be 10% of system load remains constant between the two scenarios and ranges between 60 and 120 MW.
- The thermal unit commitment is slightly lower in Scenario 2 for almost all hours.
- The down-reserves from committed thermal generation decreases in Scenario 2 during daylight hours because the PV generation causes lower dispatch levels on thermal units. There are many times during mid-day hours where committed thermal units are dispatched at, or close to, their minimum operating levels (P-Min), thus reducing the availability of down-reserves for response to over-frequency events.

---

[5] SNSP is defined by EirGrid as a measure of non-synchronous generation online as a percentage of total system demand.
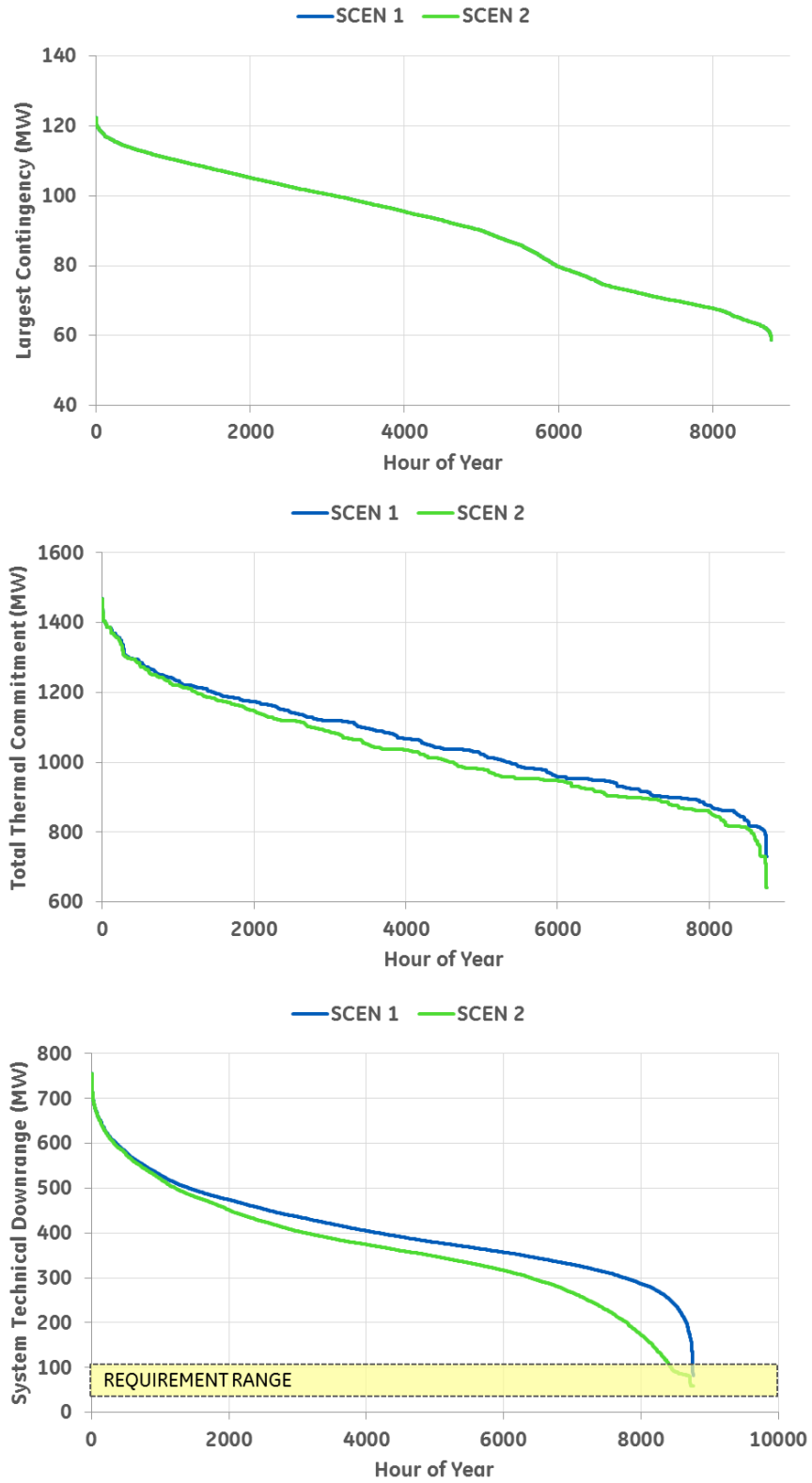
Figure 9: Hourly Duration Curves of Composite Metric Variables by Scenario

3.2 Selecting System Dispatch Conditions

The second step in the analysis included a detailed review of the production cost simulations in an effort to select certain system dispatch conditions to pass from the production cost results to the dynamic frequency response simulations. To do this each hour was quantified based on its expected risk of dynamic stability for a loss of load event. A new metric was developed that incorporated four important factors to frequency response into a single quantifiable measure. This followed the same process as the Part 1 System Frequency Response to Generator Contingency Events analysis, but used the *inverse* and opposite metric variable where necessary. On the Oahu grid, it was assumed that the following three variables would be the largest differentiators in frequency response:

1. **Largest load contingency:** It was assumed that the largest single load contingency was an immediate loss of 10% of system load, based on feedback from the technical review committee. For the purposes of this analysis it was assumed that this contingency was independent from the DPV generation, and that the load rejection did not also disconnect distributed generation. This is a conservative assumption because increasing DPV on the tripped load feeders will reduce the *net load* reduction as seen by the grid because generation on the distribution feeder will also be disconnected. Unlike the largest generator contingency event analyzed in Part 1, the largest load rejection contingency is more difficult to quantify and warrants further investigation to understand the specific failure points of the system so that appropriate mitigations can be addressed.
2. **Thermal unit commitment:** This variable was added as a proxy for system inertia and represents the amount of total capacity committed (MW) during every hour. Even if the unit is dispatched at P-min for a given hour, the unit's full rated capacity is counted as being online. The larger the thermal commitment, the more system inertia and overall grid support from conventional generators.
3. **Down-reserves online:** This variable represents the amount (MW) of frequency response available to the system. Also referred to as downrange, it is measured by taking the difference between each unit's dispatched loading and the unit's technical P-min provided in Table 1. Only thermal units with frequency response enabled (governor action) are included in this metric. The more down-reserves online, the more frequency response is available to respond to a load rejection event.

    Note: Unlike the Part 1 System Frequency Response to Generator Contingency Events analysis, *Legacy DPV generation* was not included in the composite metric calculation for the load rejection analysis. This is because a conservative assumption is made to neglect the over-frequency legacy DPV, as explained in Section 2.3 and 3.5.

In order to combine the three variables listed above into a single metric, a weighting factor (multiplier) was applied to each of the variables based on its expected influence on the magnitude and direction of system frequency in response to a generator trip event. While the same methodology was used as the Part 1 System Frequency Response to Generator Contingency Events analysis, the weighting factors differ in magnitude and direction. Therefore, the same hour dispatch will have two resulting composite metrics, one for under-

frequency events (generator contingencies) and one for over-frequency events (load contingencies). This allows for separate screening of at-risk hours for the different events.

Because the metric is meant to define system risk, the sign of the multiplier depends on each variable's likely contribution to a frequency deviation. Therefore, the largest load contingency variable is multiplied by a positive weighting factor because it is directly related to frequency deviation (the higher the variable the higher the expected frequency deviation). The thermal unit commitment and down-reserves online variables are multiplied by a negative weighting factor because they are inversely related to frequency deviation (the higher the variable the lower the expected frequency deviation).

The magnitude of the weighting factors was also related to the expected impact on system frequency and was developed to strengthen the relationship with the observed frequency response from the dynamic simulations and the calculated metric. A variable that is likely to have a larger relative impact on frequency deviation received a larger weight. The standard deviation of each variable was also taken into account when creating the weighting factors to make the scaling consistent with the overall spread of the sample size selected for dynamic simulations. These weighting factors were adjusted based on the results of the dynamic simulations in Step 3, such that the corresponding polynomial fit of the metric to the simulated frequency zenith was improved and thus provided better estimation of frequency response.

The equation below shows the mathematical formation of the metric.

$$metric = (l_i * w_l) + (c_i * w_c) + (r_i * w_r)$$

where:

l is the size of the largest load contingency.
c is the amount of committed thermal unit capacity.
r is the amount of down-reserves online.
i is the observation of each variable for a given hour of the year.
w is the weighting factor applied to each variable.

The following tables provides an example of the metric calculation for two hours of the year in Scenario 1. This calculation shows the difference between a high risk hour (2534) and a lower risk hour (3091). The resulting metric in the high risk hour is 1.97 whereas the resulting metric in the lower risk hour is -6.82. Relative to hour 2534, hour 3091 has a higher thermal unit commitment and higher down-reserves online. As a result, even with the higher system load and larger contingency, the metric (system risk) is significantly lower. While the number itself does not have any direct meaning, it provides a relative measure for system risk for all hours over the course of the year. A higher metric indicates larger expected frequency deviation during a load trip event, and therefore higher system stability risk.

Table 4: Metric Calculation Example, Hour 2534, Scenario 1

Hour 2534	Largest Contingency (MW)	Thermal Unit Commitment (MW)	Down-Reserves Online (MW)	Summed Metric
Observation	84.35	731.80	15.92	
Weight	0.0700	-0.0050	-0.0175	
Weighted Score	5.91	-3.66	-0.28	1.97

Table 5: Metric Calculation Example, Hour 3091, Scenario 1

Hour 3091	Largest Contingency (MW)	Thermal Unit Commitment (MW)	Down-Reserves Online (MW)	Summed Metric
Observation	108.03	1386.40	425.43	
Weight	0.0700	-0.0050	-0.0175	
Weighted Score	7.56	-6.93	-7.45	-6.82

The metric calculation shown in the examples above was performed for each hour of the year based on the chronological production cost simulation results from Section 3.1. The resulting metric provides a screening analysis for system risk across each hour of the year. Figure 10 illustrates the average and maximum metric by hour of the day for both scenarios. In general, the metric, and therefore the system risk and expected frequency deviation, is highest during the mid-day (high solar) hours. The early morning and evening hours are least at risk because additional thermal units are online just before and after the daily net-load ramps and thus provide more governing response than in other hours. Unlike the Part 1 System Frequency Response to Generator Contingency Events analysis, increasing DPV causes the metric to increase during mid-day hours because the additional solar de-commits thermal generators, without reducing the system load risk. The impact on thermal unit commitment is somewhat muted because the additional reserve requirement associated with the increased DPV requires units to stay online during solar output periods.
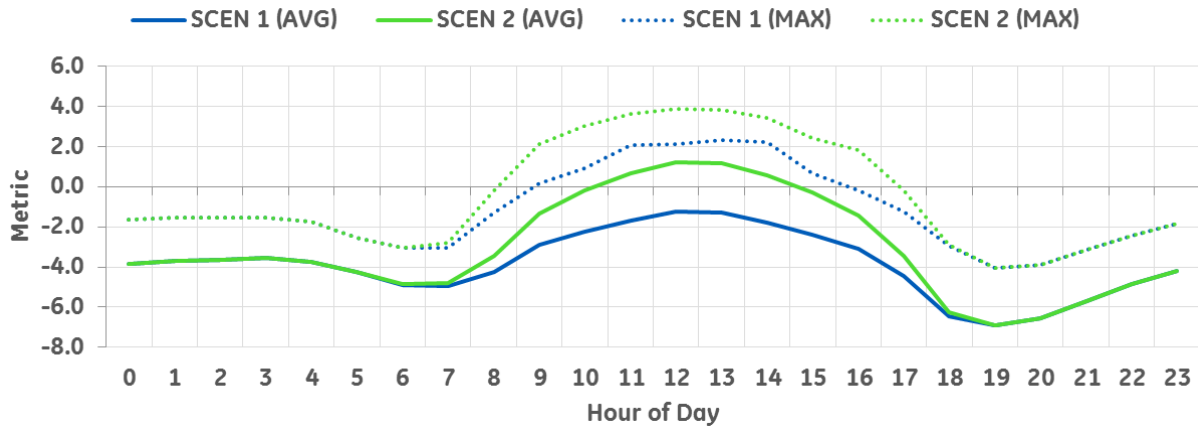
Figure 10: Average and Maximum Metric by Hour of the Day, Scenario 1 & 2

Using the 8,760 hourly results from a year of simulation completed in Step 1 (Section 3.1) and the metric calculation discussed above, each hour of the year can be ranked from highest expected risk to lowest based on the system dispatch conditions for any given hour. The resulting duration curves are provided in Figure 11 and were created by sorting each hour of the year from highest to lowest based on the calculated metric. From the 8,760 dispatch conditions, a sample of 15 dispatch conditions in each scenario was selected in order to simulate in the dynamic frequency response simulations (Section 3.3) and thereby validate the metric's overall ability to estimate system frequency deviations due to load rejection events. The original 13 selections are consistent with the Part 1 System Frequency Response to Generator Contingency Events analysis to allow for direct comparison of dispatch conditions between the two contingency events. An additional two hour selections were evaluated to include the hour with the highest value for the metric to ensure the most challenging dispatch conditions in both scenarios were evaluated. The individual hour validation points are highlighted in Figure 11. The dispatch conditions for each validation point, including each generator's power output, overall system load, and DPV generation was passed from the production cost simulations to the dynamic frequency response simulations, as described in the following section.
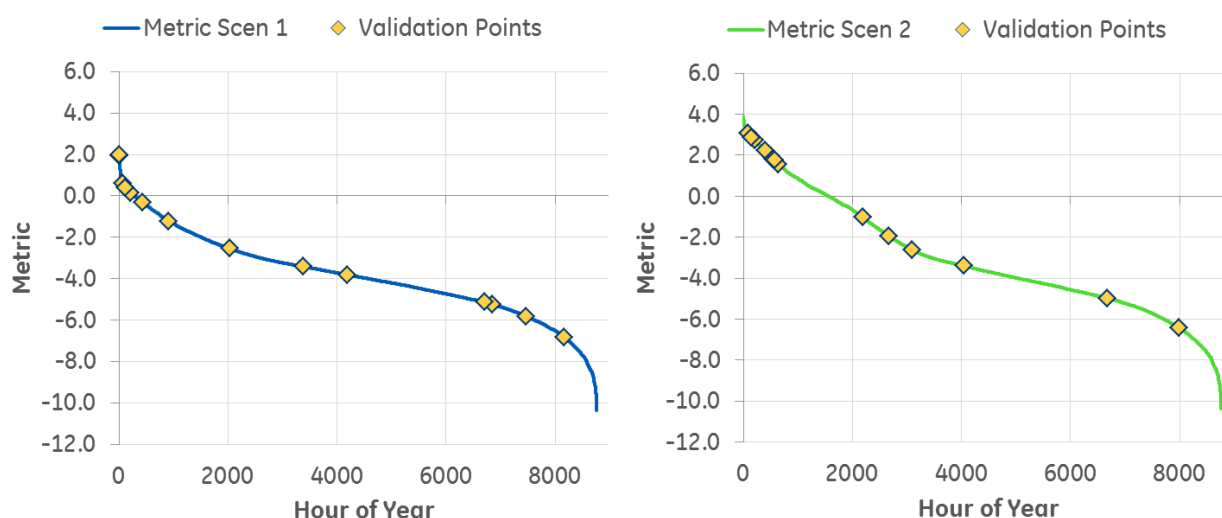
Figure 11: Hourly Metric Duration Curve with Selected Validation Points

3.3 Dynamic Frequency Response Simulations

The dispatch conditions for each selected hour from Step 2 were incorporated into the GE PSLF model for further dynamic simulations. The load, generator output, and distributed PV was setup for each dispatch condition and allocated to individual power flow busses, with full representation of the transmission network model.

In Scenario 1 for example, Hour 3519 (Saturday, May 27th, 2:00 PM) in the production cost simulations was determined to be the most challenging for a load rejection event based on the metric calculation. During this hour, the system load was 935.8 MW (not including house loads at the generators) and DPV output was 233 MW (58% of nameplate capacity). The unit

dispatch for that time hour is shown in Figure 12. Note that Kahe 6 was offline due to a scheduled maintenance or forced outage event. Under this dispatch condition, the 10% loss of load event was a 93.6 MW contingency.

Unit Name	Dispatch (MW)
AES	180.0
Kahe 1	0.0
Kahe 2	25.0
Kahe 3	35.2
Kahe 4	0.0
Kahe 5	45.0
Kahe 6	0.0
Waiau 3	0.0
Waiau 4	0.0
Waiau 5	0.0
Waiau 6	0.0
Waiau 7	33.4
Waiau 8	25.0
Waiau 9	0.0
Waiau 10	0.0
Kalaeloa 1	90.0
Kalaeloa 2	90.0
Kalaeloa 3	0.0
CIP-CT	0.0
AIR-DSG	0.0
H-Power	68.5
Wind	30.4
CPV	80.6
DPV	232.8
System Load	935.8
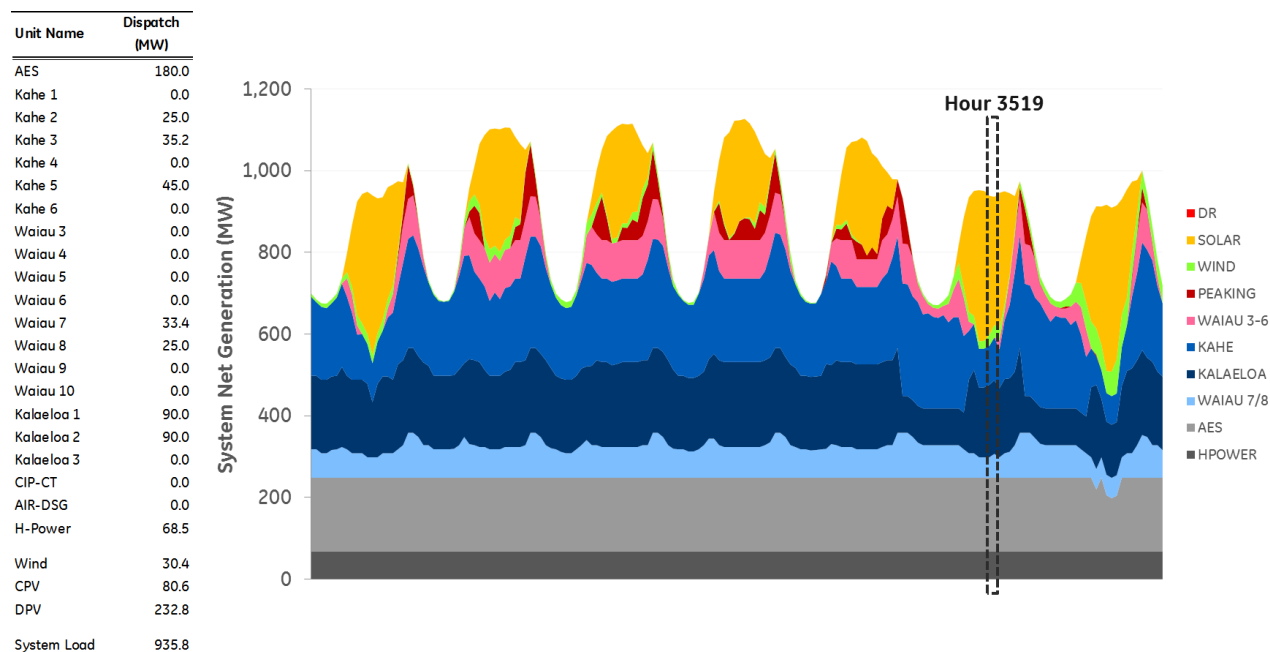
Figure 12: System Dispatch Conditions for Hour 3519, Scenario 1

The results of the dynamic simulation are provided in Figure 13 and Figure 14. From the figure, the following observations can be made:

- The loss of system load during that hour (10% = 93.6 MW), which was triggered in the dynamic simulation at Time = 10 seconds, causes system frequency to increase rapidly
- During this time, the output of the thermal generators decreases in an effort to balance system generation with load, and thereby stop the increase in frequency.
- Eventually the rising frequency arrests at the frequency zenith of 61.60 Hz and begins its backswing, and reaches a new stable equilibrium approximately 15 seconds after the generator contingency.
- AGC and system operator controls later restore system frequency to 60 Hz after the new stable equilibrium is reached.

Oahu Network Simulation
System Response to a Load Trip, No Droop on Renewables
Scenario 1, Hour 3519
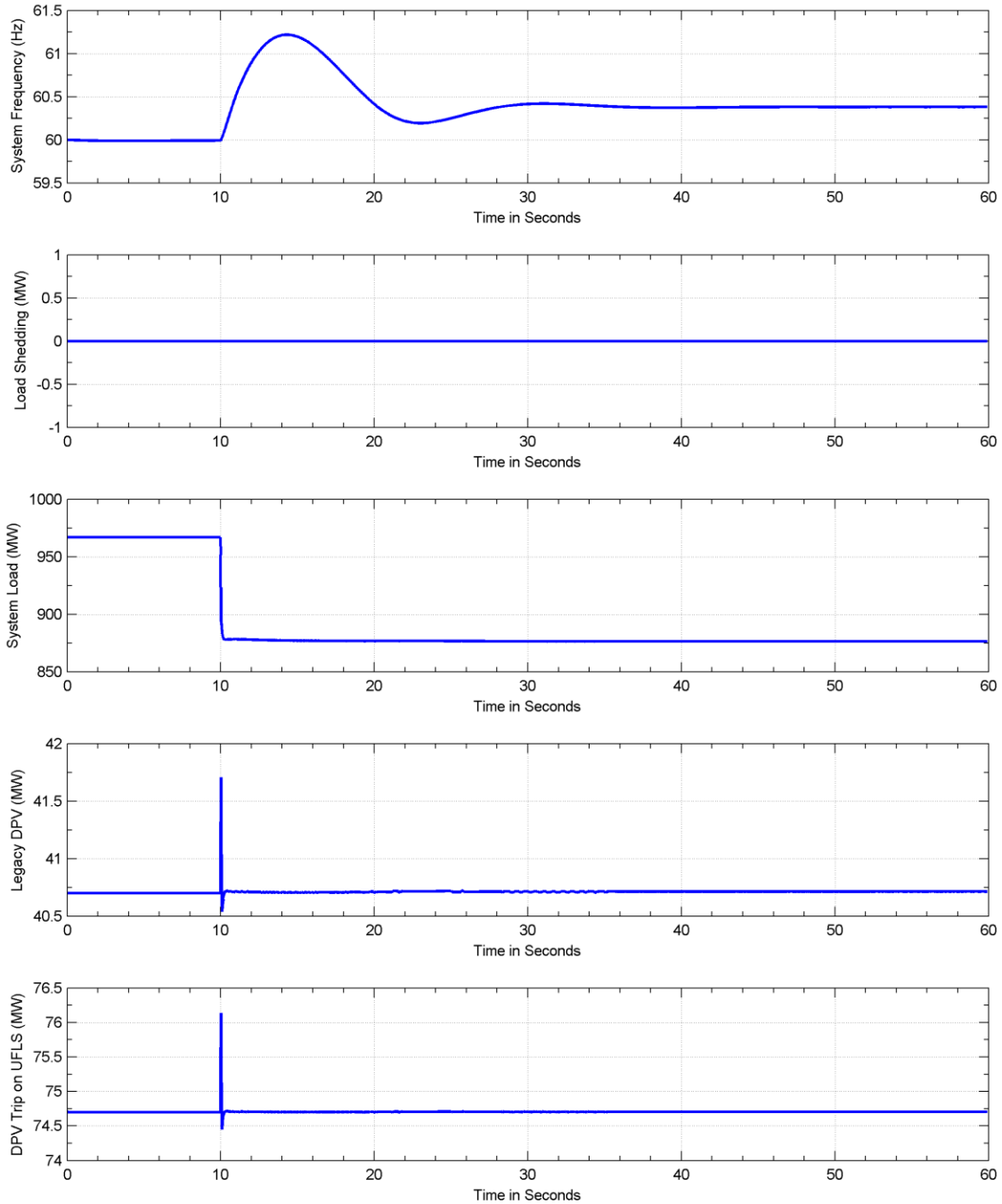
Figure 13: Dynamic Simulation Results (I), Hour 3519, Scenario 1
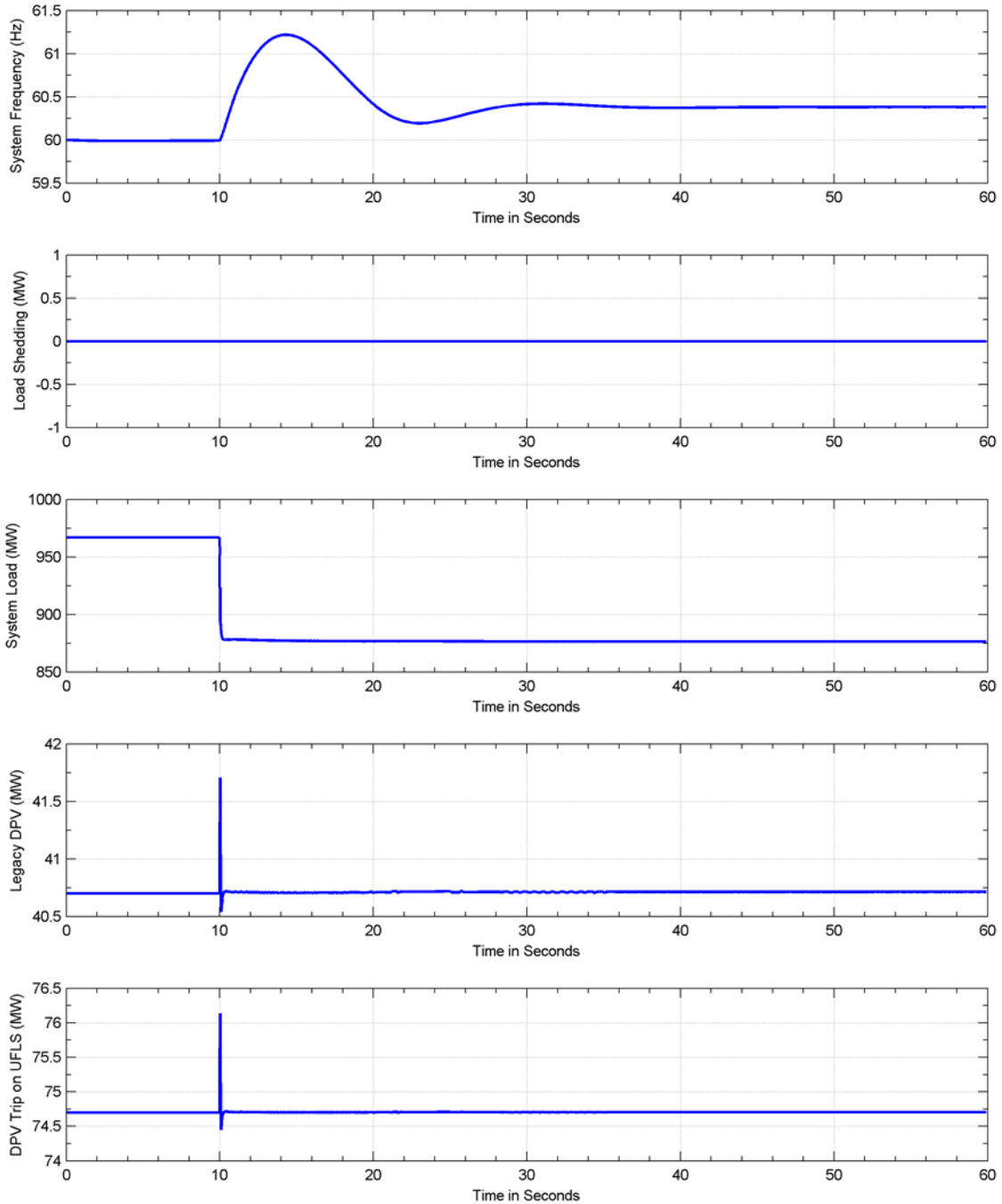
Figure 14: Dynamic Simulation Results (II), Hour 3519, Scenario 1

The dynamic simulation was also performed on the same hour in Scenario 2. The additional 300 MW of DPV capacity resulted in an additional 174.6 MW of DPV generation online during the hour. Given the same amount of system load, the additional DPV generation displaced generation from other generators on the system and is shown in Table 6. Kahe 2 was cycled offline, Kahe 3, Kalaeloa CC and Waiau 7 reduced generation to P-Min, and AES generation was reduced by 81 MW. This displacement was determined by the production cost simulations and based on system economics and other operational constraints. At this point all thermal generators remaining online, with the exception of AES, were must-run units dispatched at P-min.

Table 6: System Dispatch Conditions for Hour 3519, Scenario 1 vs Scenario 2

Unit Name	SCEN 1 (MW)	SCEN 2 (MW)	DELTA (MW)
AES	180.0	99.0	-81.0
Kahe 1	0.0	0.0	0.0
Kahe 2	25.0	0.0	-25.0
Kahe 3	35.2	25.0	-10.2
Kahe 4	0.0	0.0	0.0
Kahe 5	45.0	45.0	0.0
Kahe 6	0.0	0.0	0.0
Waiau 3	0.0	0.0	0.0
Waiau 4	0.0	0.0	0.0
Waiau 5	0.0	0.0	0.0
Waiau 6	0.0	0.0	0.0
Waiau 7	33.4	25.0	-8.4
Waiau 8	25.0	25.0	0.0
Waiau 9	0.0	0.0	0.0
Waiau 10	0.0	0.0	0.0
Kalaeloa 1	90.0	65.0	-25.0
Kalaeloa 2	90.0	65.0	-25.0
Kalaeloa 3	0.0	0.0	0.0
CIP-CT	0.0	0.0	0.0
AIR-DSG	0.0	0.0	0.0
H-Power	68.5	68.5	0.0
Wind	30.4	30.4	0.0
CPV	80.6	80.6	0.0
DPV	232.8	407.4	174.6
System Load	935.8	935.8	0.0

Under these new conditions, the load contingency was held constant at 93.6 MW, despite the increased DPV on the system. Total thermal commitment was reduced by 82 MW (Kahe 2), and the down-reserve provision decreased by 100 MW. The frequency response of the system is shown in Figure 15 for the same hour in both Scenario 1 and Scenario 2. With the reduced system inertia from Kahe 2 being offline and the reduced down-reserve available on the remaining thermal units, the net frequency deviation increased. The frequency zenith in Scenario 2 was 61.78 Hz, 0.53 Hz higher than the zenith in Scenario 1.
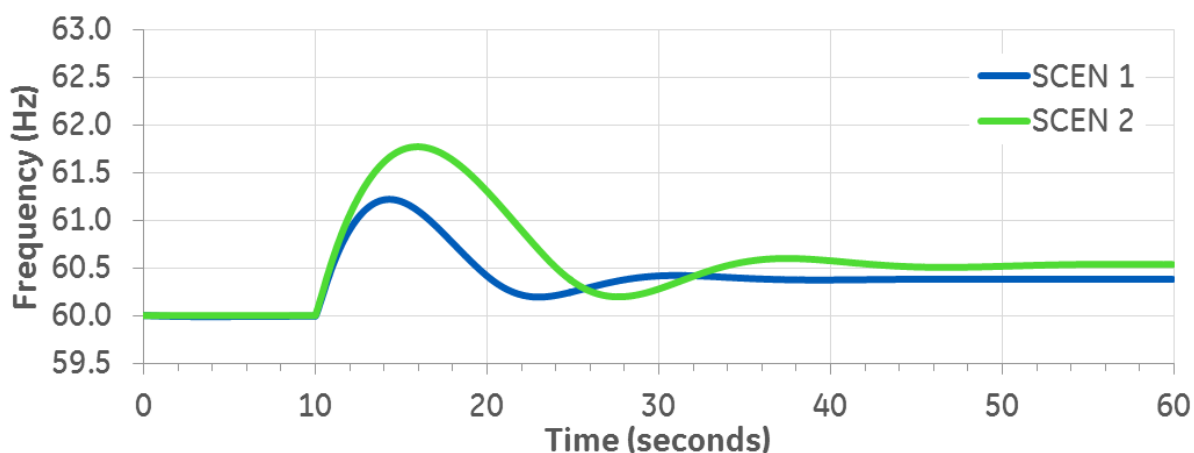
Figure 15: System Frequency Response for Hour 3519, Scenario 1 vs Scenario 2

The magnitude and severity of the frequency excursion depends largely on the extent to which thermal generators are cycled offline (reduced system inertia) and reduced down-range on the remaining online generators. For example, all the thermal units shown in Figure 16 respond to the load rejection in Scenario 1. But in Scenario 2, Kahe 3 is already dispatched at P-min when the load rejection occurs so its governor is not able to reduce power further, and the other thermal units must compensate with larger responses. Figure 16 provides the corresponding thermal generator responses to the load rejection event.

Unit commitment and dispatch can change significantly over the course of the year depending on system load and renewable resource conditions. Therefore it is important to look at multiple operating points over the course of a year and develop a holistic view of system stability. To ensure this, the dynamic simulations were repeated for each of the 15 dispatch conditions selected in Step 2 (Section3.2) for each scenario.

Oahu Network Simulation
System Response to a Load Trip, Scen 1 (Blue) and Scen 2 (Green)
Hour 3519
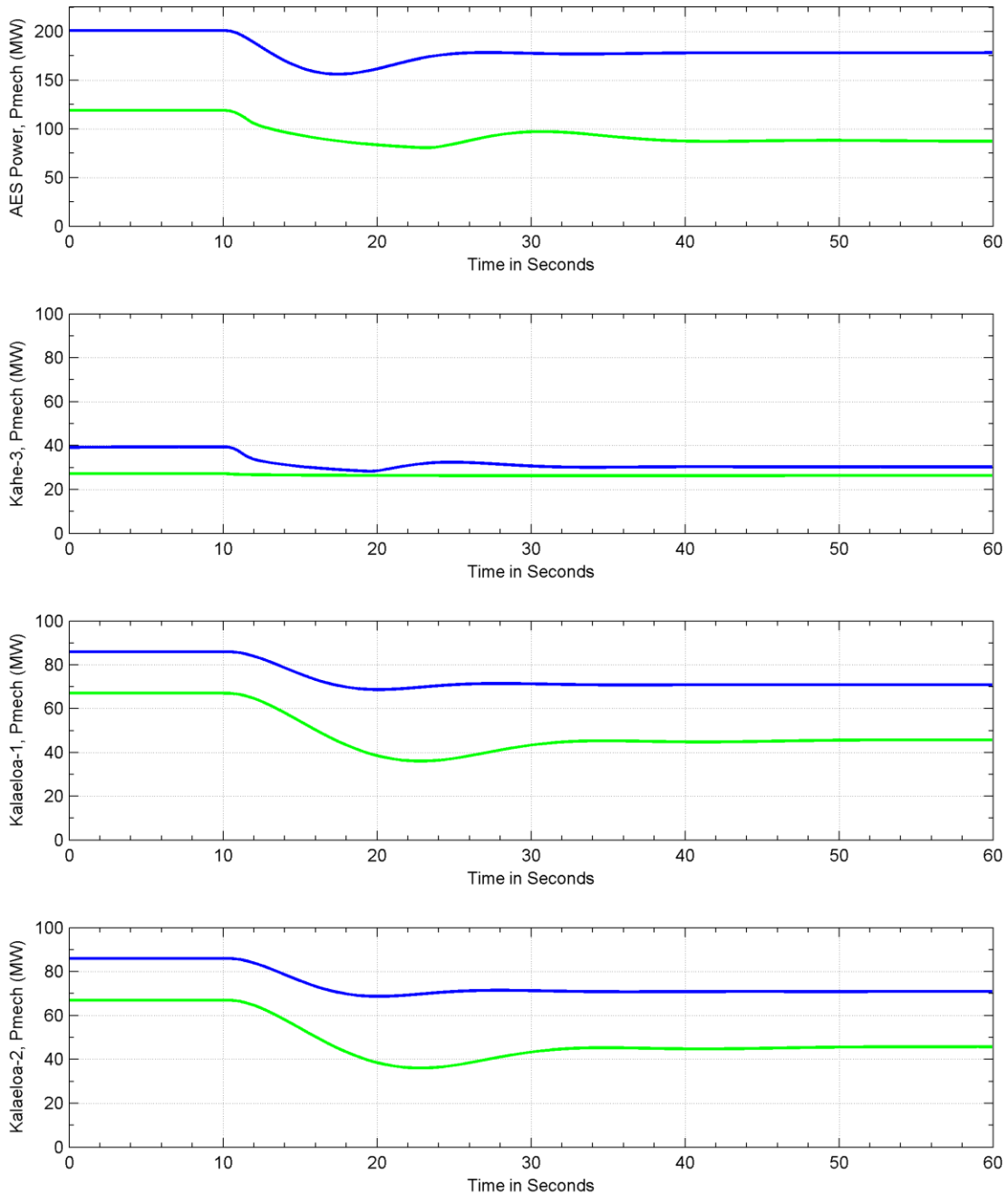
Figure 16: Response of Thermal Units for Hour 3519, Scenarios 1 and 2

The results of each simulation are provided in the Appendix, with a summary of the frequency zenith and frequency deviation provided Table 7 for both Scenario 1 and Scenario 2. While the only change in the scenario composition is the amount of DPV capacity on the system, the increased dispatch from the DPV for any given hour may cause secondary changes to the commitment and dispatch of other thermal units on the system. From the table it can be observed that the relationship between the metric and the observed frequency deviation is confirmed between Scenarios 1 and 2. As the metric increases from Scenario 1 to Scenario 2, the simulated frequency deviations also increase and stability deteriorates.

Table 7: Observed Frequency Response from Dynamic Simulations

Hour	SCENARIO 1			SCENARIO 2		
	Metric	Zenith (Hz)	Deviation (Hz)	Metric	Zenith (Hz)	Deviation (Hz)
2534	2.0	62.00	2.00	2.2	62.40	2.40
1597	0.6	61.60	1.60	3.1	62.70	2.70
2340	0.4	61.60	1.60	2.9	62.50	2.50
1095	0.2	61.56	1.56	2.8	62.50	2.50
3519	-0.3	61.25	1.25	1.8	61.78	1.78
5604	-1.2	61.00	1.00	1.6	61.75	1.75
8074	-2.5	60.88	0.88	-1.0	61.05	1.05
634	-3.4	60.80	0.80	-2.0	60.90	0.90
7649	-3.8	60.75	0.75	-2.6	60.72	0.72
4482	-5.1	60.65	0.65	-3.4	60.80	0.80
1184	-5.3	60.68	0.68			
402	-5.8	60.68	0.68	-5.0	60.65	0.65
3091	-6.8	60.68	0.68	-6.4	60.68	0.68
6087				1.8	61.75	1.75
2197	1.9	62.60	2.60	1.9	62.60	2.60

3.4 Estimating Frequency Response

Using the results from the 28 dynamic frequency response simulations (14 in Scenario 1 and 14 in Scenario 2), the final step of the analysis investigated the relationship between the metric developed in Step 2 with the observed frequency response metrics calculated in Step 3. As discussed earlier, the metric was designed to exhibit a direct relationship between the metric and system stability; the higher the metric, the higher the expected frequency deviation and system risk following a load rejection event. Figure 17 shows the relationship of system frequency deviation (dependent variable) as a function of the metric (independent variable) for each of the 28 dynamic simulations conducted in Step 3. This was done for both Scenario 1 (blue markers) and Scenario 2 (green markers) to see the relationship between the frequency zenith and metric with increasing DPV penetration. A polynomial best-fit trend line was then calculated for the 28 operating points as the equation below.

$$y = 0.0019x^3 + 0.0402x^2 + 0.2818x + 61.332$$

where x is the composite metric and y is the expected frequency zenith
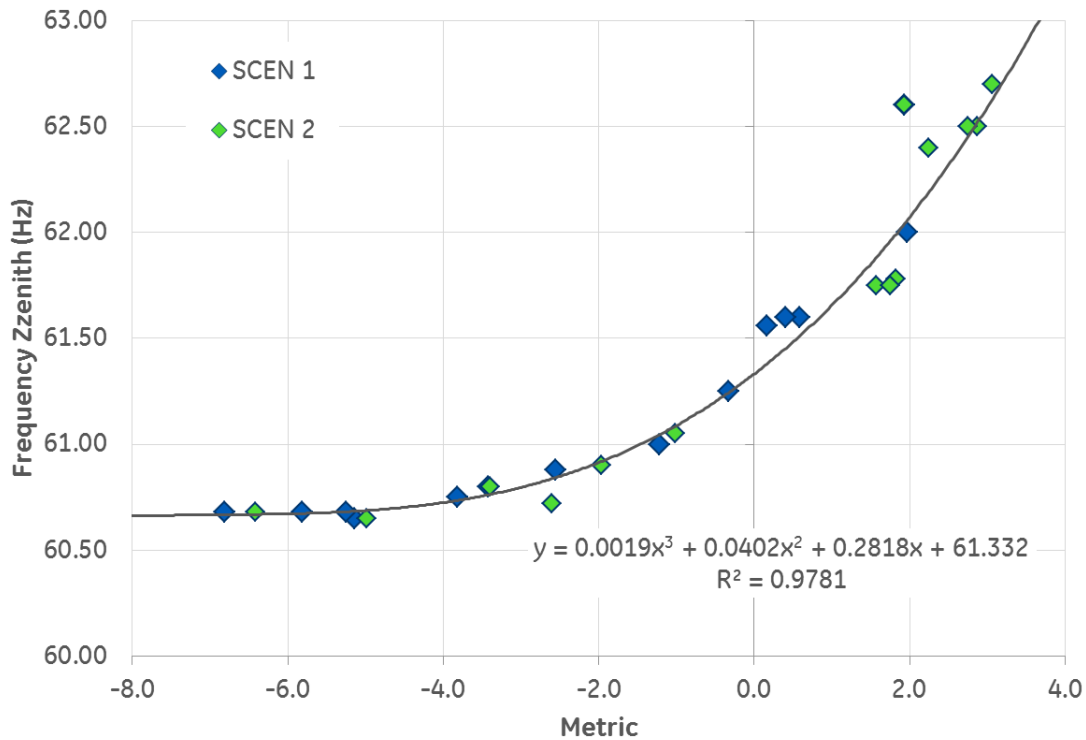
Figure 17: Regression of Frequency Zenith as a Function of the Metric

Note that this used the same methodology as the Part 1: System Frequency Response to Generator Contingency Events analysis, but with the updated metric, new dynamic simulations, and a resulting new polynomial best fit line. The curve-fit for the load rejection analysis trends upward, showing that an increased metric (system risk) results in a higher frequency zenith (frequency deviation).

The chart also highlights several dispatch conditions that exhibit significant system risk, with six observations where the frequency zenith is above 62 Hz. The clustering of green data points in the upper right quadrant of the charts visually highlights the increased system risk in Scenario 2, with increased levels of DPV penetration. The cubic best fit trend line can be used to estimate the frequency nadir, frequency deviation and UFLS for any metric value (and thus system dispatch condition), without the need for additional dynamic frequency response simulations. This was done for all 8,760 hours in both Scenario 1 and Scenario 2. By doing this, the overall system risk was estimated under each system dispatch condition, thereby providing a better understanding of trends between scenarios and under different operating conditions. In addition, it allows the reader to draw conclusions about the probability or frequency of different operating conditions, as opposed to traditional stability analysis that only evaluates the most extreme operating points that may only occur rarely throughout the year.

Figure 17 and Figure 18 show the expected magnitude and probability of a frequency deviation for a load rejection event for each hour of the year based on an entire year of system operation. The duration curves in Figure 17 sort the expected frequency deviations from highest to lowest while the histogram in Figure 18 quantifies the number of hours in a year where the system is expected to be operating in a range of frequency deviations given a load rejection event. The duration curves are also separated for daytime hours (with DPV online) and nighttime hours (without DPV). From these charts it can be observed that:

- There is a clear difference between the expected frequency deviation during daytime and nighttime operating periods and the magnitude of this difference becomes larger with more DPV online.
- For nearly all daytime hours, the frequency deviation for a load rejection event in Scenario 2 (700 MW DPV) is significantly greater than in Scenario 1 (400 MW DPV)
- The number and severity of the largest frequency deviations also increases, highlighting more operating conditions of increased risk with higher DPV penetration.
- While the grid is expected to remain stable and avoid system collapse over the course of a full year of operation, there are several hours where the system frequency zenith approaches levels where protective actions could trip generation resources due to over-frequency.
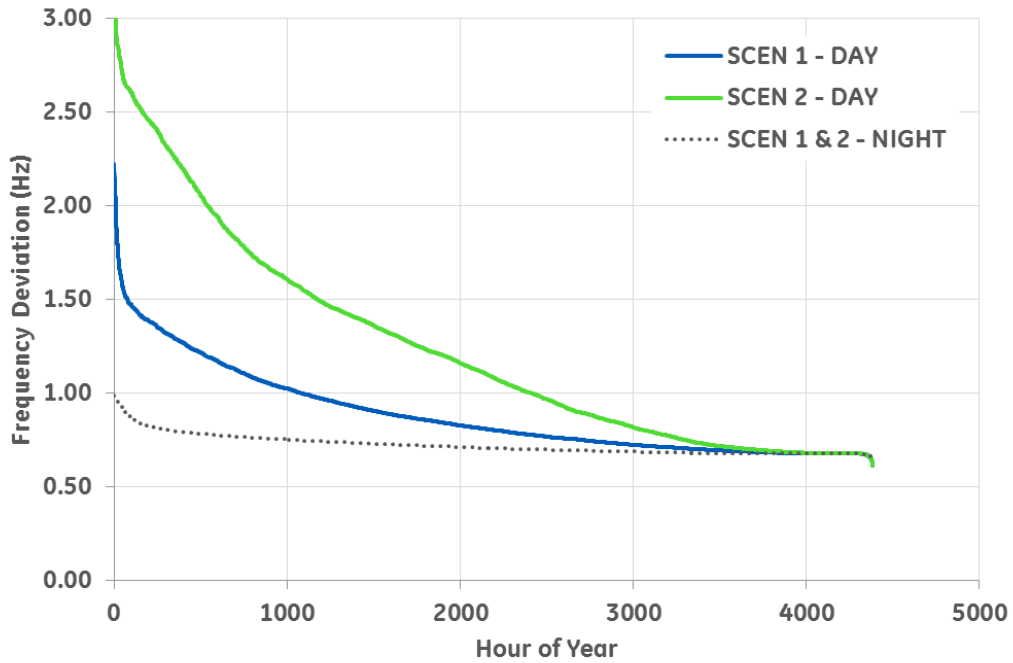
Figure 18: Duration Curve of Expected Frequency Deviation by Scenario
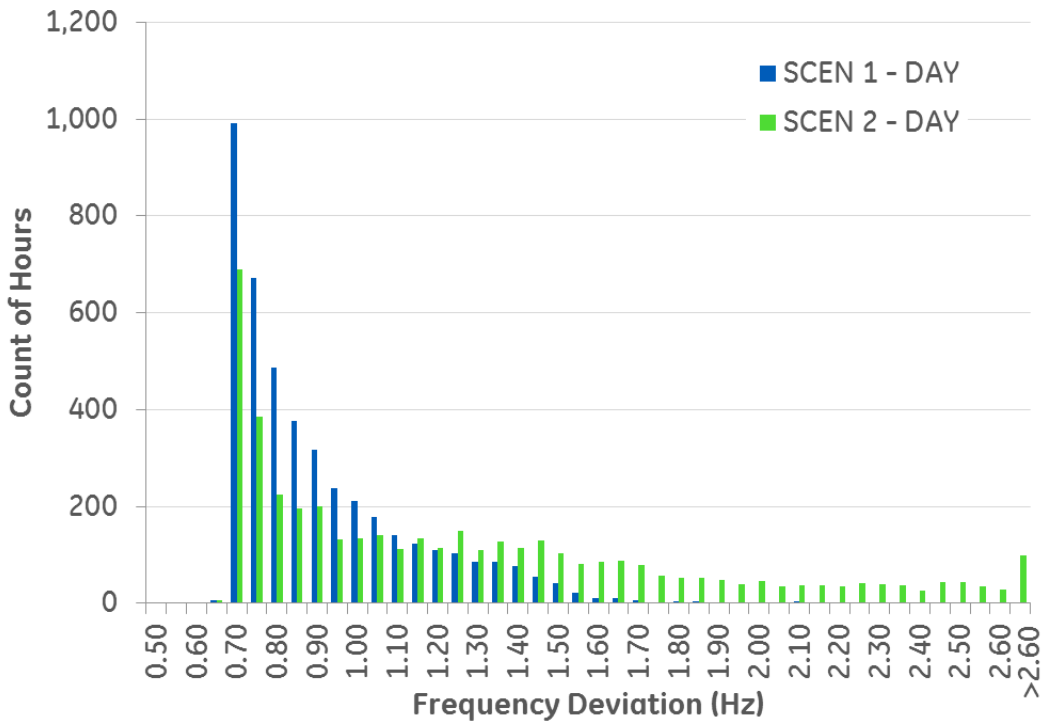
Figure 19: Histogram of Expected Frequency Deviations by Scenario

3.5 Sensitivity to Over-Frequency Trip Settings on Legacy DPV

Oahu presently has 106 MW of legacy DPV generation that will trip if the system frequency exceeds 60.5 Hz. This sensitivity analysis examines the possible changes to overall grid frequency response due to that legacy DPV.

The impact of legacy DPV setting on system frequency for load rejection (over-frequency) contingency events is primarily determined by the magnitude (MW) of load tripped relative to the magnitude (MW) of DPV generation tripped immediately following the loss of load. Three conditions are considered:

1. No Legacy DPV generation is tripped after a loss of load event (Base Case)
2. MW Legacy DPV generation tripped < MW load tripped
3. MW Legacy DPV generation tripped > MW load tripped

The analysis presented in Sections 3.3 and 3.4 assumed that no legacy DPV is tripped after a loss of load event (a conservative assumption). This is similar to having over-frequency ride-through on all DPV, including the legacy DPV.

If the amount of tripped legacy DPV generation is small with respect to the loss of load (for instance, during a cloudy period), then the generating assets with governors respond by reducing power output, but to a smaller degree as the small amount of legacy DPV generation that trips will help the system frequency to recover. An example is shown in Figure 20, where the loss of load of 96 MW is quickly offset by a loss of DPV generation of 76 MW (estimated legacy DPV production at the time of the event), which causes system frequency to return to the nominal value faster than if the legacy DPV generation had not tripped. Although this faster recovery is a "silver lining" to the "gray cloud" of improper DPV frequency protection settings, it is not recommended to intentionally operate in this manner as tripping of generation resources is a non-linear and potentially destabilizing means of grid frequency control.

If the MW of generation tripped is greater than the initiating MW of load tripped, then the net effect is similar to a loss of generation event, which can be severe if generation lost greatly exceeds load lost. In Oahu, the worst case would require:

1. A complete loss of 106 MW of DPV generation under the assumption that all legacy DPV is operating at peak output, and
2. A minimum loss of load such that the system frequency still triggers the 60.5Hz frequency threshold.

The minimum loss of load required to reach 60.5Hz may be estimated from Figure 17, where even the least severe event reaches 60.6Hz. Thus a 10% loss of load is a reasonable value. If an average system load value of 900MW is assumed, then the minimum loss of load event that would still trigger the 60.5Hz threshold would be 90 MW. To the system, this would appear to be a net 16 MW loss of generation contingency. From the Part 1 analysis of generation contingencies, this is a very mild contingency that would not trigger any UFLS. Therefore, even the most severe effect due to over-frequency legacy DPV settings does not threaten grid stability or UFLS at a level of 106 MW, and so the assumption to neglect the over-frequency tripping of legacy DPV is conservative.
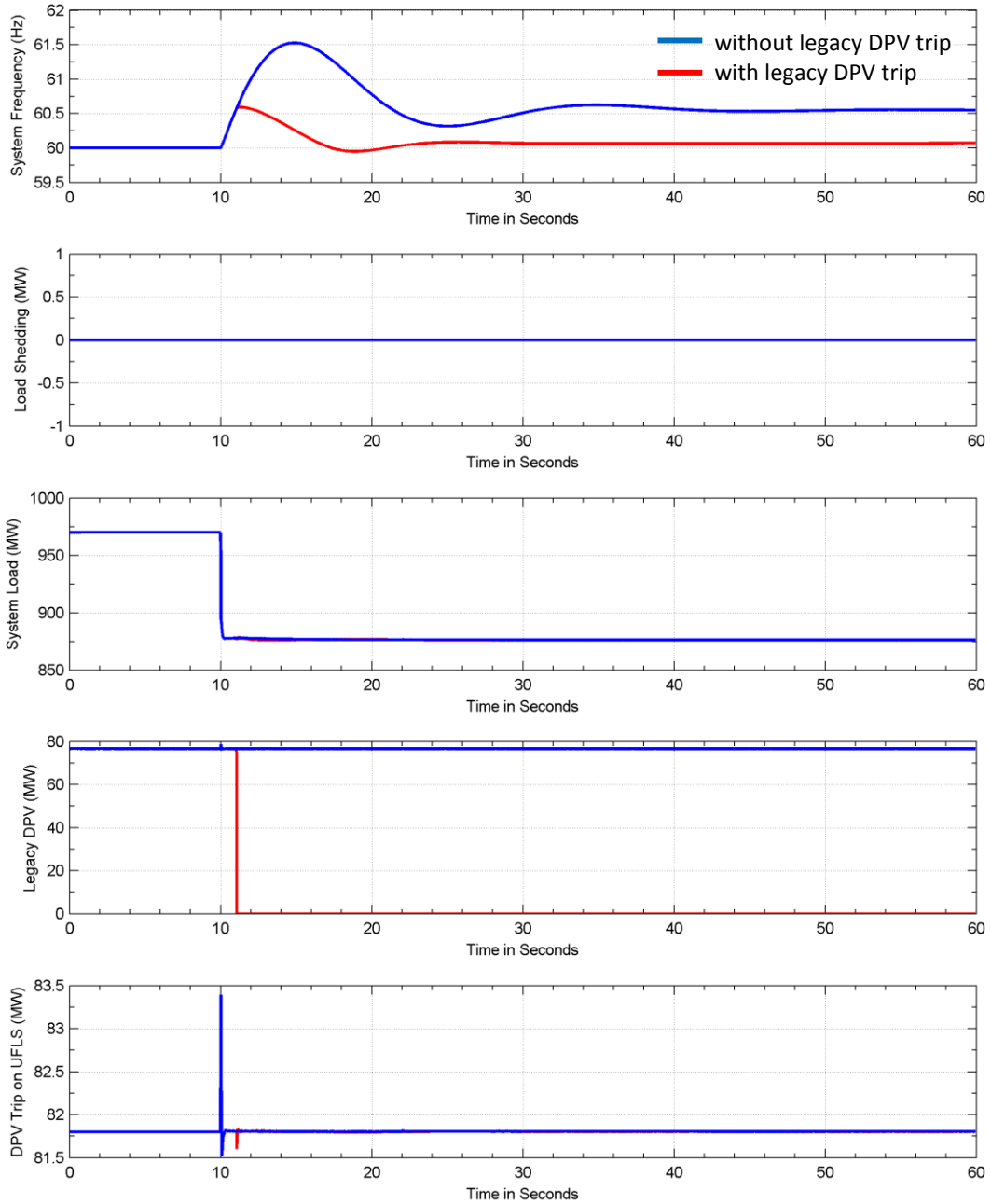
Figure 20: System Response with and without Legacy DPV Over-frequency Ride-Through

4 MITIGATIONS AND RECOMMENDATIONS

4.1 Overview of Frequency Response from Wind and Solar

The results of the previous section showed that absent mitigations, the expected frequency deviation to a load rejection event increased significantly with increased DPV penetration on the system. This occurs because under current operating practices, the down-reserves allocated to respond to over-frequency events are carried only by conventional thermal units. As generators are decommitted, system inertia is reduced and fewer conventional units are online to provide frequency governor response. Procuring additional down-reserves from conventional thermal units would require additional unit commitment or higher minimum operating levels. Both of these options would result in increased wind and solar curtailment, decreased system operating efficiency, and increased system operating costs.

As a result, it is important to look to new sources of ancillary services, like primary frequency response, to maintain grid stability. While these new sources could include energy storage, demand response, electric vehicles, and other grid upgrades, utilizing the existing wind and solar on the system for primary frequency response is a viable mitigation that requires little capital cost and upgrades for the utility scale plants. With proper controls and infrastructure, over-frequency response could be supplied by distributed generation resources as well.

With appropriate controls, wind and solar generators are capable of providing primary frequency response for a load rejection event (using frequency droop or frequency-watt control features). Both wind and solar resources are capable of quickly reducing power output in response to a grid over-frequency event through governor action, thereby augmenting the response of governors on the conventional power plants. In fact, the power-electronic converters within the wind and solar generators are capable of changing power output at rates that are significantly faster than conventional thermal plants with steam-turbines or combustion turbines, which depend on mechanical actuators to control steam flow or fuel flow.

Because the load rejection events are rare and have a short duration involved with frequency response (tens of seconds), there is no material impact on total energy production or plant economics. Unlike under-frequency response, there is no opportunity cost of forgone generation that the generators must incur to provide this service, making it an attractive ancillary service procurement strategy for the system operator.

The rest of this section provides an overview of over-frequency primary frequency response from wind and solar along with results from two sensitivities listed below (sensitivity A refers to the Base Case assumptions discussed throughout the previous sections):

- Sensitivity B: Over-frequency governor droop on utility scale wind and solar
- Sensitivity C: Over-frequency governor droop on utility scale wind and solar, as well as distributed PV.

The purpose of this analysis is to demonstrate the changes to grid frequency response and the services that wind and solar resources can provide to maintain grid stability. The analysis

was split into two sensitivities because although the over-frequency droop is technically possible on the DPV, the necessary control systems to coordinate thousands of distributed resources is not yet in place and warrants further investigation. In addition, this analysis assumes that ALL distributed PV has over-frequency droop capability. While it is recognized that some of the legacy inverters will not have this capability, the case was used as an upper bound of the frequency response capability.

4.2 Dynamic Frequency Response Simulations with Mitigations

In order to quantify the effect of adding over-frequency droop to the renewable fleet, each of the 28 previously analyzed dynamic simulations were rerun with updated control assumptions for the renewable plants. This process was repeated twice, once for each sensitivity, allocating governor response across different resources. The only change incorporated to the dynamic simulations was the over-frequency droop assumption; all other system and plant parameters (load, generator dispatch, contingency stimulus, etc.) were held constant to allow for direct comparison of the results.

The frequency response of the system following a 10% load contingency is again shown in Figure 21, this time also incorporating over-frequency droop on the renewables. The dispatch conditions originate from Hour 3519, the same conditions as shown previously in Figure 15. The green line, SCEN 2A, represents the base case assumptions and the same frequency trace previously shown. The yellow line, SCEN 2B, represents the frequency response with over-frequency droop on the utility scale renewables only, and the red line, SCEN 2C represents the frequency response with over-frequency droop on the utility scale renewables and distributed solar, DPV. The solid lines all represent results from Scenario 2, with 700 MW of installed DPV capacity. The dotted grey line is provided for reference and represents the original frequency response trace from Scenario 1 (400 MW DPV) from the original base case analysis depicted as the blue line in Figure 15.

Figure 22 shows the governor response of individual thermal units and Figure 23 shows the aggregated response of all wind plants, all central PV plants, and all DPV. The colors of the traces are consistent with Figure 21. Note that the governor on Kahe 3 is unable to reduce power output because the unit is already dispatched at minimum power, P-min., at the time of the load rejection event.
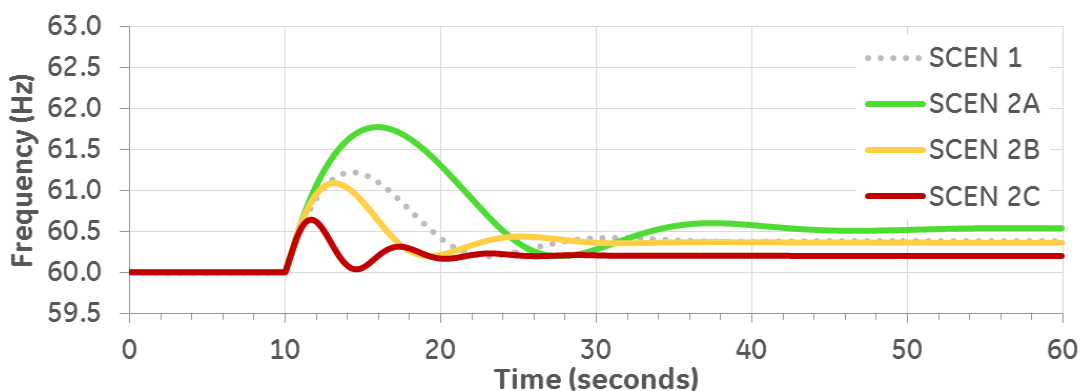
Figure 21: System Frequency Response for Hour 3519, Scenario 2, with Mitigations

Oahu Network Simulation
System Response to a Generator Trip, Rnwb Droop Green (0), Yellow (Cen), Red (Dist)
Scenario 2, Hour 3519
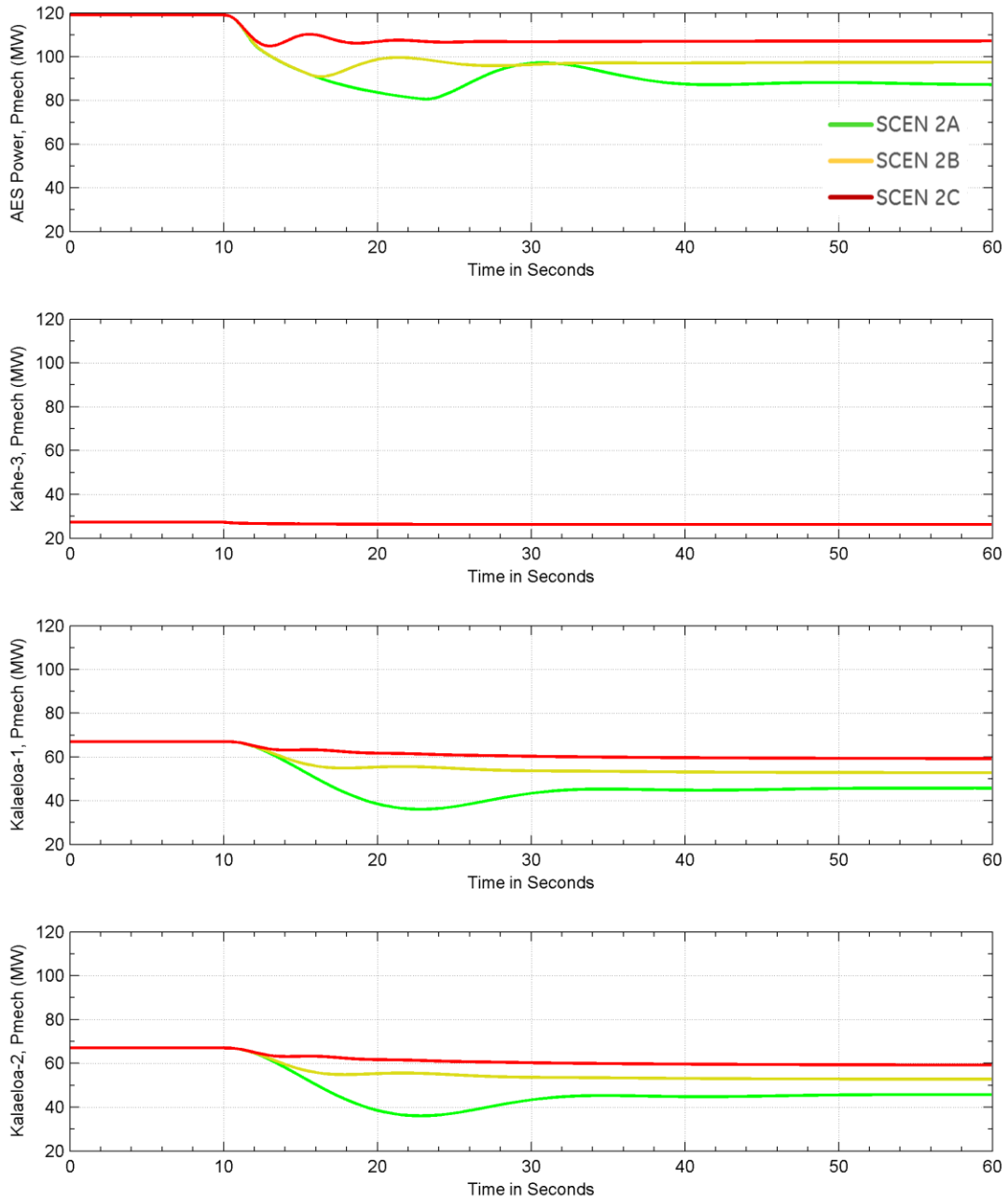
Figure 22: Response of Thermal Units for Hour 3519, Scenario 2, with Mitigations
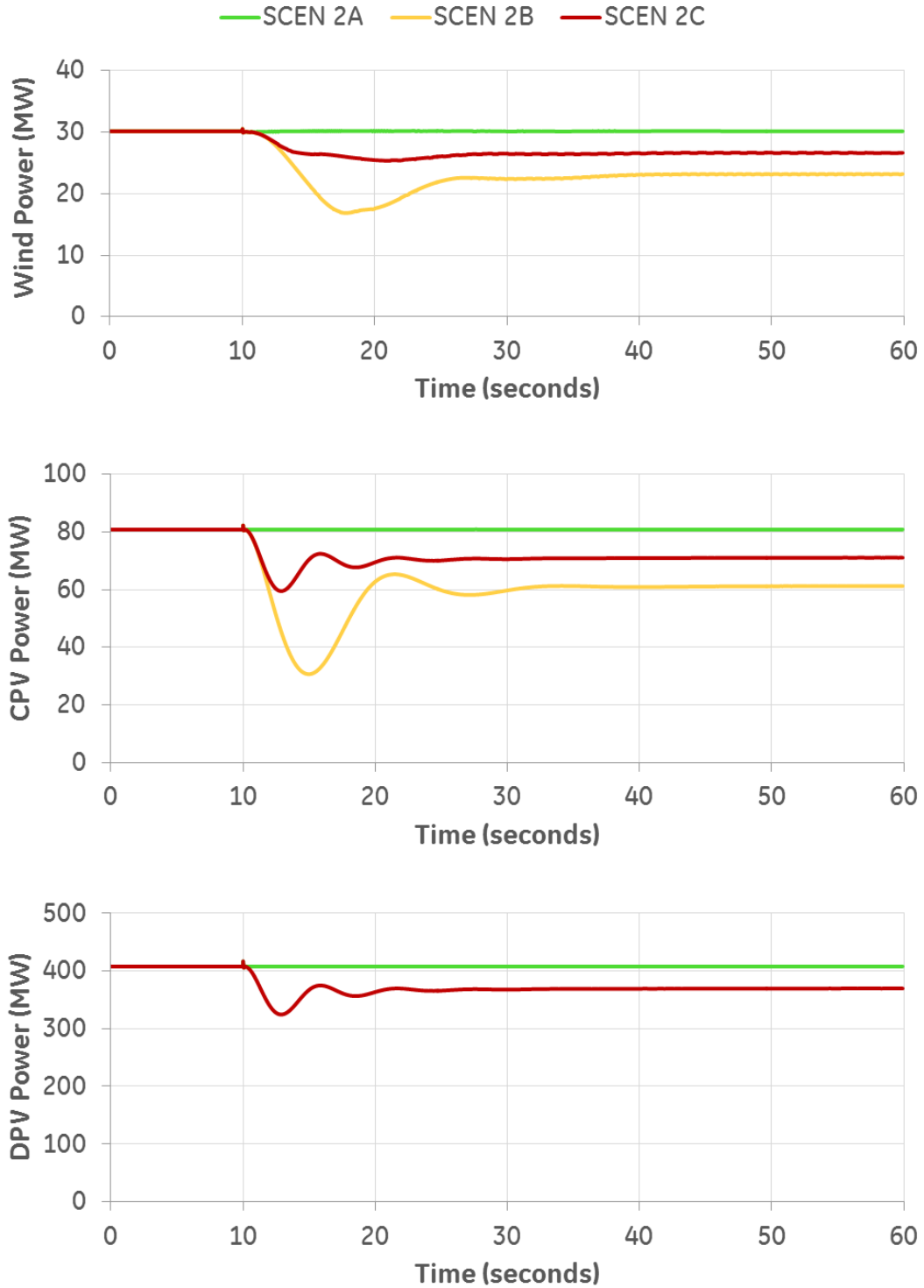
Figure 23: Aggregated Response of Renewable Resources,
Hour 3519, Scenario 2, with Mitigations

Several observations can be made related to the system frequency response following a load rejection event, with and without over-frequency droop on the renewables:

- The initial rate of change of frequency (RoCoF) in the 1-2 seconds immediately following the contingency stimulus does not change significantly. RoCoF (Hz/s) is measured by the initial upward-slope of the curve following the contingency. This does not change because the thermal unit dispatch is consistent across the sensitivities, and thus system inertia is unchanged. In the sensitivities, the assumption changed governor droop control only, and did not incorporate potential synthetic inertia from wind and solar inverters.

- The frequency zenith, the highest point in the frequency deviation, is significantly reduced with over-frequency droop included on wind and PV resources. in fact, the magnitude of the frequency excursion for Scenario 2 with these mitigations is smaller than the original Scenario 1 results, even with an additional 300 MW of DPV on the system.

- The frequency deviation in SCEN 2C, with over-frequency droop incorporated on the DPV as well as the utility-scale resources, is 70% lower than the base case assumption -- a very significant improvement in the grid's response.

- The system frequency backswing occurs sooner and system frequency is restored to a new stable equilibrium faster when over-frequency droop is enabled on the renewables. The new stable equilibrium is also closer to the nominal system frequency of 60 Hz.

- With wind and PV resources contributing to the grid's over-frequency governor response, the magnitude of the governing duty by thermal units is significantly reduced (see Figure 22). This is an important benefit, since it is technically challenging for a thermal unit to rapidly reduce its output to a level that approaches its technical minimum power limit. Even with well-tuned controls, there may be some risk of control issues that lead to an unintended trip of the unit.

- With more resources sharing over-frequency governing, the governing duty on each individual resource is proportionally smaller. Furthermore, the grid becomes less sensitive to the unavailability or failure to respond of any given resource. With only thermal units providing over-frequency governor response, the failure of one unit to respond would significantly increase the duty on the other thermal units.   With wind and PV sharing the duty, the impact is significantly smaller.

Similar dynamic simulations were performed for each of the 28 dispatch conditions (14 for Scenario 1 and 14 for Scenario 2) across all three mitigation sensitivities for a total of 84 dynamic simulations. The resulting frequency zenith from each simulation is provided in Table 8 along with the composite metric of system risk. These results are shown in Figure 24, which graphs the frequency zenith for each dynamic simulation in Scenario 2, with and without the over-frequency droop mitigations. A marker of the zenith in Scenario 1 is also shown as a reference to highlight the differences in frequency response when DPV is added to the system. This chart indicates that although frequency deviation increases significantly

in Scenario 2 with increasing DPV penetration, this challenge can be mitigated effectively to levels at or below the Scenario 1 Reference Case by implementing over-frequency droop on renewable resources.

Note that for two hours simulated, 2197 and 2534, the frequency zenith does not change between SCEN2A and SCEN2B. This is because all of the utility-scale renewables are curtailed during that period, leaving only DPV available. While the base case results indicated that the grid could survive the load rejection events evaluated, even without over-frequency droop on wind and solar plants, the over-saturation of DPV could become a concern at higher penetration levels. This also represents a limitation of exclusive DPV renewable growth rather than a balanced renewable resource portfolio. In Scenario 2, there were 13 hours (out of 8,760) of high DPV solar penetration where the curtailment of all utility scale wind and solar generation was required. During these times, the utility scale wind and solar cannot provide primary over-frequency response to load rejection events (although they would be able to provide primary under-frequency response to generator trip contingencies). If DPV increases further, the regularity of these events will increase. This highlights the need for controllable DPV resources by the grid operator to allow for curtailment if necessary and to provide primary frequency response from the DPV inverters, in place of the curtailed utility-scale plants. Absent this control, other mitigations would be required, such as further reduction of the thermal unit minimum operating levels (P-Min), energy storage, or demand response.

Table 8: Frequency Zenith from Dynamic Simulations, by Scenario and Sensitivity

Hour	SCENARIO 1				SCENARIO 2			
	Metric	Zenith A	Zenith B	Zenith C	Metric	Zenith A	Zenith B	Zenith C
2197	1.9	62.60	61.35	60.85	1.9	62.60	62.60	60.78
2534	2.0	62.00	61.10	60.75	2.2	62.40	62.40	60.74
1597	0.6	61.60	61.12	60.80	3.1	62.70	61.75	60.80
2340	0.4	61.60	61.10	60.78	2.9	62.50	61.75	60.75
1095	0.2	61.56	61.10	60.76	2.8	62.50	61.35	60.70
3519	-0.3	61.25	60.90	60.65	1.8	61.78	61.10	60.64
5604	-1.2	61.00	60.85	60.70	1.6	61.75	61.25	60.73
8074	-2.5	60.88	60.70	60.58	-1.0	61.05	60.78	60.52
634	-3.4	60.80	60.68	60.54	-2.0	60.90	60.75	60.53
7649	-3.8	60.75	60.65	60.55	-2.6	60.72	60.72	60.52
402	-5.8	60.68	60.60	60.50	-5.0	60.65	60.60	60.45
3091	-6.8	60.68	60.60	60.50	-6.4	60.68	60.60	60.47
4482	-5.1	60.65	60.57	60.50	-3.4	60.80	60.68	60.50
1184	-5.3	60.68	60.67	60.65				
6087					1.8	61.75	61.25	60.74
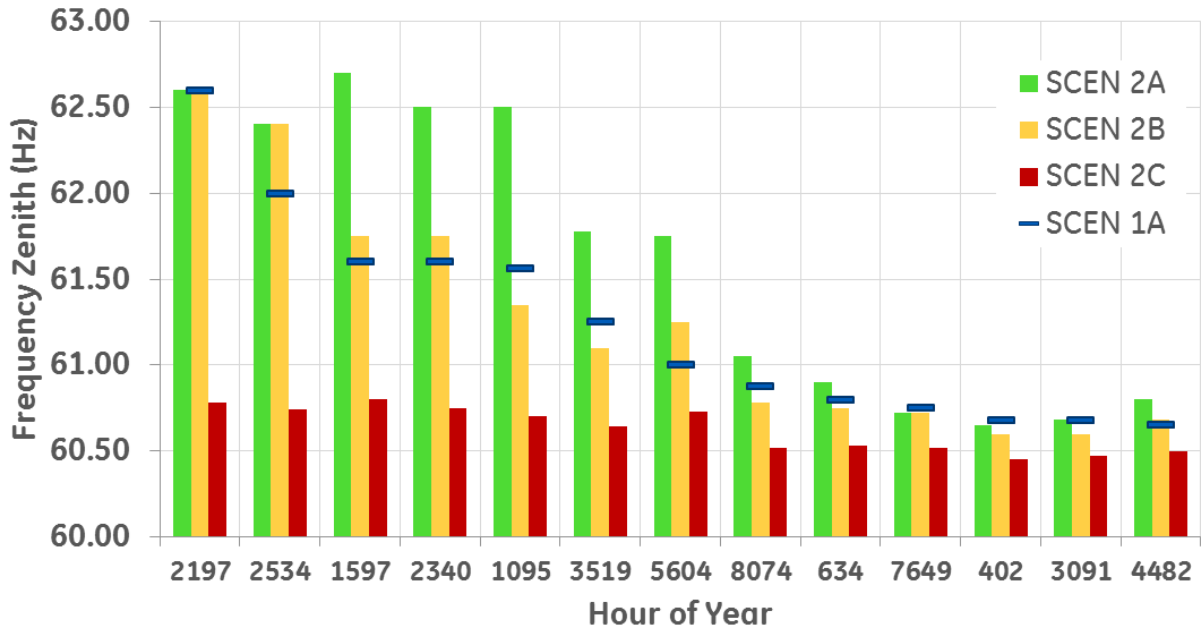
Figure 24: Frequency Zenith from Dynamic Simulations, by Scenario and Sensitivity

4.3   Estimating Frequency Response with Mitigations

Using the same methodology as the base case analysis, the results of the frequency response simulations can be used to quantify a relationship between the metric developed in Step 2 with the observed frequency response metrics calculated in Step 3. In the sensitivity analysis the underlying function is expected to change due to the incorporation of the renewable over-frequency droop. Using the results from the 84 dynamic frequency response simulations, the results were again plotted against the original composite metric.

Figure 25 shows the relationship of system frequency deviation (dependent variable) as a function of the metric (independent variable) for each of the dynamic simulations conducted. This was done for both Scenario 1 (blue markers) and Scenario 2 (green markers) to see the relationship between the frequency zenith and metric with increasing DPV penetration, as well as each sensitivity: diamonds represent the original base case assumption with over-frequency droop on the thermal resources only, the circles represent Sensitivity B with over-frequency response added to utility-scale renewables, and the triangles represent Sensitivity C, with over-frequency droop added to both utility-scale and distributed renewables. Three separate polynomial best-fit trend lines were then calculated for each sensitivity, and a new function was calculated to estimate system frequency response with and without the over-frequency droop mitigation.
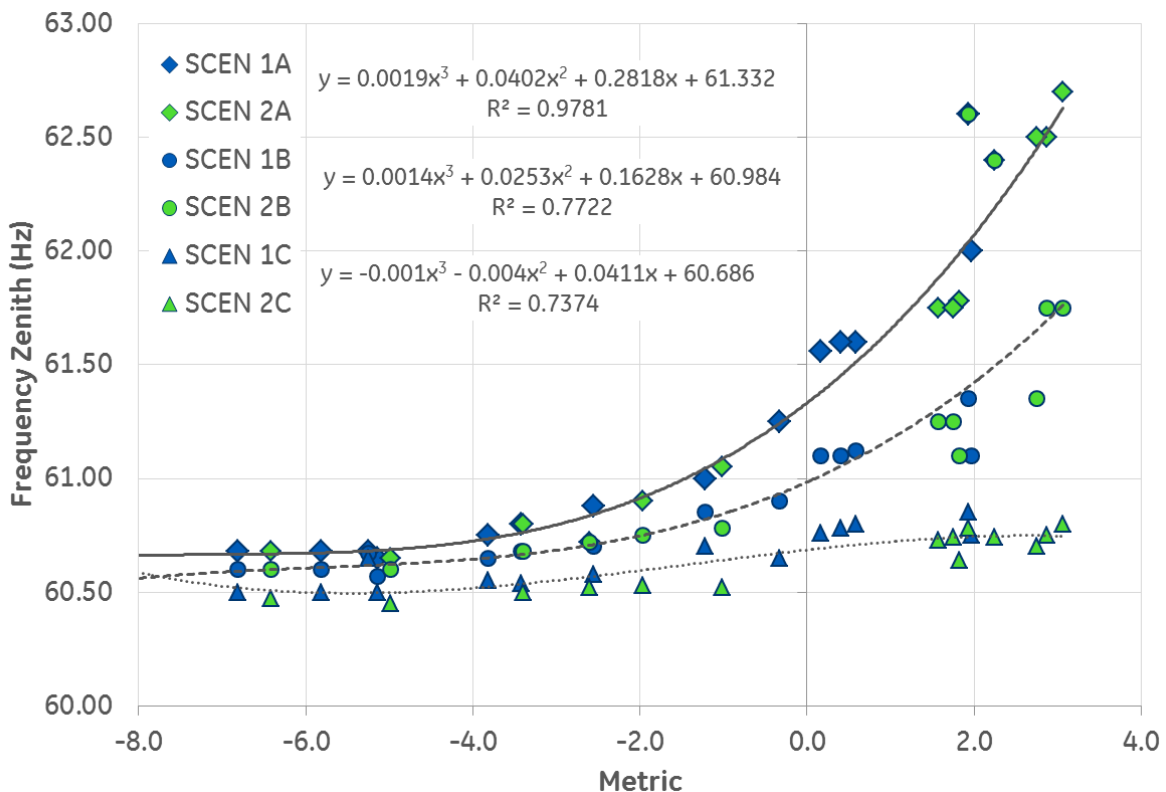
Figure 25: Regression of Frequency Zenith as a Function of the Metric, by Sensitivity

As shown in Section 3.4, the equations shown in Figure 25 can again be used to estimate the expected frequency deviation across the entire year of operation, with and without frequency response provided by the utility-scale and distributed renewable generation. This provides a better understanding of how system risk changes over the course of the year as DPV penetration increases, but also quantifies how much of that risk can be mitigated by implementing over-frequency governor controls on the wind and solar generators. Figure 26 shows duration curves of the estimated daytime frequency deviation by sensitivity for Scenario 2, with the original Scenario 1 base case estimation also provided in grey as a reference point. From this chart it can be determined that:

- As discussed earlier in this report, the estimated over-frequency deviation increases significantly when more DPV is added to the system, absent other mitigations. This is measured by the increased duration curve from Scenario 1A (grey dotted line) to the Scenario 2A curve (green line).
- Adding over-frequency droop capability to the utility-scale renewables decreases the expected frequency deviation to the yellow curve, which is at approximately the same level as the Scenario 1 base case.
- Extending the over-frequency droop capability to the DPV resources further reduces the expected frequency deviation to the red line, which is relatively flat. This shows that system risk to over-frequency load rejection events is not a significant concern throughout the year with this mitigation enabled.
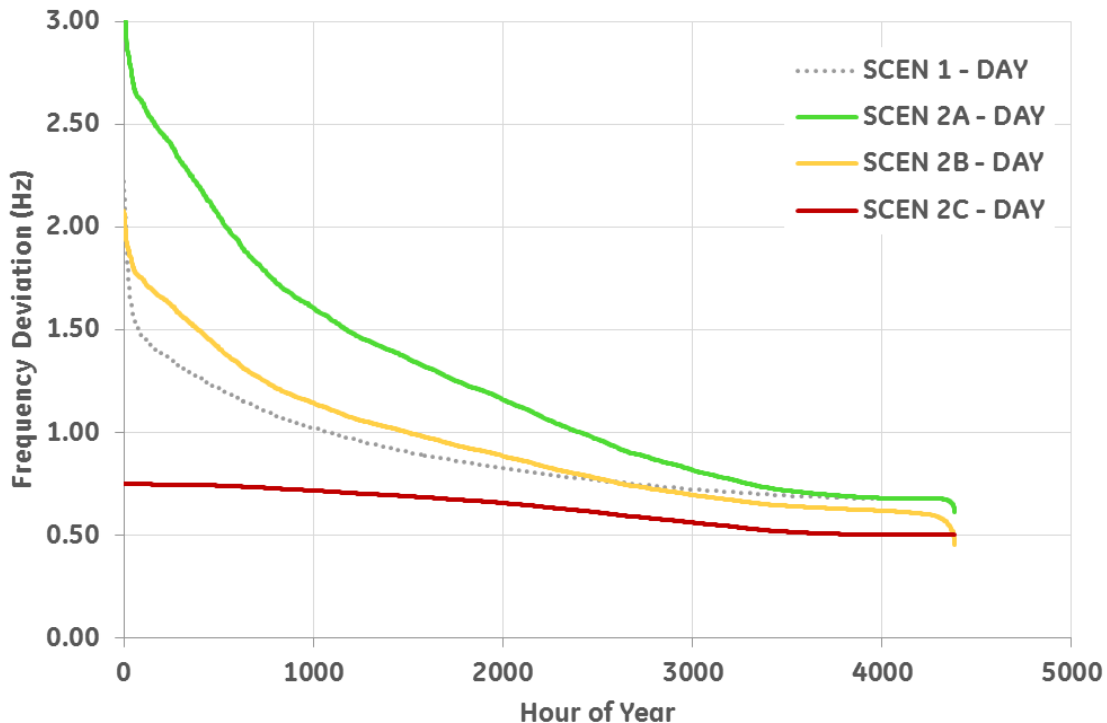
Figure 26: Duration Curve of Expected Frequency Deviation by Sensitivity

5 KEY FINDINGS

5.1 Important Observations

The results of this study provide useful insights to the stable and reliable growth of DPV on the Oahu power grid. However, the following observations should be viewed in the broader context of the study scope and limitations stated previously. In addition, the trends and observations highlighted in this study were based on a system with 700 MW of DPV, 150 MW of CPV and 124 MW of wind. Extrapolating results beyond the renewable penetration studied in this analysis should not be done without further technical analysis.

- While the grid is expected to remain stable and avoid system collapse over the course of a full year of operation, there are several hours where the system frequency zenith approaches levels where protective actions could trip generation resources due to over-frequency absent other operational changes.

- Unlike the largest generator contingency event analyzed in Part 1, the source and magnitude of largest load contingency is more difficult to pinpoint and quantify. As a result, a better understanding of the load rejection risk warrants further investigation so that appropriate mitigations can be addressed.

- The down-reserves from committed thermal generation decreases in Scenario 2 during daylight hours because the PV generation causes lower dispatch levels on thermal units. There are many times during mid-day hours where committed thermal units are dispatched at, or close to, their minimum operating levels (P-Min), thus reducing the availability of down-reserves for response to over-frequency events.

- In general the system risk and expected frequency deviation, is highest during the mid-day (high solar) hours. The early morning and evening hours are least at risk because additional thermal units are online just before and after the daily net-load ramps and thus provide more governing response than in other hours.

- There is a clear difference between the expected frequency deviation during daytime and nighttime operating periods and the magnitude of this difference becomes larger with more DPV online.

- Several dispatch conditions evaluated were operating under conditions that exhibit significant system risk, with six of the 28 simulation cases having a frequency zenith above 62 Hz. Most of these points occur in Scenario 2, with increased levels of DPV penetration.

- As generators are decommitted, system inertia is reduced and fewer conventional units are online to provide frequency governor response. Procuring additional down-reserves from conventional thermal units would require additional unit commitment or higher minimum operating levels. Both of these options would result in increased wind and solar curtailment, decreased system operating efficiency, and increased system operating costs.

- It is important to look to new sources of primary frequency response, to maintain grid stability. While these new sources could include energy storage, demand response, electric vehicles, and other grid upgrades, utilizing the existing wind and solar on the system for primary frequency response is a viable mitigation that requires little capital cost and upgrades for the utility scale plants, and with proper controls and infrastructure could be supplied by distributed generation resources as well.

- Adding over-frequency governor controls to wind and solar generating resources can effectively augment the governing action of conventional generation and significantly improve the system's ability to withstand load rejection events with increased penetration of DPV generation.

- There are a few hours of the year when central wind and solar plants are curtailed to an extent where the over-frequency governing response from those plants is either partially reduced or totally unavailable. Although it is anticipated that this may be a small effect for a limited number of hours, further analysis is required to quantify the impacts of wind and solar curtailment on the effectiveness of this mitigation approach.

5.2 Future Research

While the analysis outlined throughout this report provides valuable insight to grid stability concerns on Oahu with increasing DPV, other questions critical to assessing grid stability remain. It is therefore suggested that the following items be evaluated in future study work, as the islands strive forward towards meeting the RPS goals. Much of this material will be covered in future stages of this study using a similar modeling approach and project team.

- **Short Circuit Ratios:** As the penetration of grid-connected power electronic equipment like wind, central & distributed PV, and storage increases, the electrical "stiffness" of the grid tends to decrease, which could lead to voltage and control instabilities on the grid. Because the risk of instability is highly dependent on the electrical stiffness of the grid, which can change suddenly and many times a day, the instantaneous renewable penetration is often used as a proxy for this risk. This analysis will quantify the short-circuit strength of the Oahu grid under various expected operating conditions to help assess the risk of power electronic equipment instability.

- **Synthetic Inertia:** The over-frequency droop mitigation evaluated in this study simulated governor controls only and did not evaluate the capability of renewables, storage, or demand response to provide synthetic inertia. Synthetic inertia would improve the stability of the grid for contingency events like generation and load trips by providing a fast-responding, stabilizing injection or absorption of power at the onset of the event and should be evaluated further.

- **Higher Renewable Penetration:** While this study evaluated a doubling of solar capacity on Oahu, annual wind and solar energy penetration remained below 25% and well below future RPS targets. Scenarios with higher renewable penetration must be evaluated to determine frequency response at higher penetration.

- **Evaluate Different Systems:** The quadratic equation formulated in this study proved to be a good predictor of frequency response. However it is unique to the current Oahu grid configuration. As the thermal resource mix on Oahu changes or this analysis is extended to neighboring islands, the metric needs to be recalibrated based on additional dynamic simulations.

- **Grid Support from Wind & Solar:** While not evaluated in this study, curtailed utility-scale wind and solar can provide under-frequency governor response for generator trip events. While curtailing wind and solar specifically to provide this ancillary service may not be economic, utilizing already curtailed generation due to other constraints could increase grid security.

- **Examine Mitigations:** Although grid stability with increasing DPV penetration can be effectively mitigated with over-frequency droop controls, several additional mitigations should be evaluated to improve frequency response, reduce UFLS, and increase grid stability. Such mitigations could include demand response, energy storage, electric vehicles, dynamic UFLS schemes, minimum number of units online, and spinning reserve adjustments.